Yersinia Type III-Secreted Effectors Evade the Caspase-4 Inflammasome in Human Cells

Jenna Zhang[a], Igor E. Brodsky[b,#], and Sunny Shin[a,#]

[a]Department of Microbiology, University of Pennsylvania Perelman School of Medicine, Philadelphia, Pennsylvania 19104

[b]Department of Pathobiology, University of Pennsylvania School of Veterinary Medicine, Philadelphia, Pennsylvania 19104

Running title: *Yersinia* evades human inflammasome activation

#Co-corresponding authors: Igor E. Brodsky ibrodsky@vet.upenn.edu and Sunny Shin sunshin@pennmedicine.upenn.edu

Abstract word count: 170

Text word count: 4781

Abstract

Yersinia are gram-negative zoonotic bacteria that use a type III secretion system (T3SS) to inject *Yersinia* outer proteins (Yops) into the host cytosol to subvert essential components of innate immune signaling. However, *Yersinia* virulence activities can elicit activation of inflammasomes, which lead to inflammatory cell death and cytokine release to contain infection. *Yersinia* activation and evasion of inflammasomes have been characterized in murine macrophages but remain poorly defined in human cells, particularly intestinal epithelial cells (IECs), a primary site of intestinal *Yersinia* infection. In contrast to murine macrophages, we find that in both human IECs and macrophages, *Yersinia pseudotuberculosis* T3SS effectors enable evasion of the caspase-4 inflammasome, which senses cytosolic lipopolysaccharide (LPS). The antiphagocytic YopE and YopH, as well as the translocation regulator YopK, were collectively responsible for evading inflammasome activation, in part by inhibiting *Yersinia* internalization mediated by YadA and β1-integrin signaling. These data provide insight into the mechanisms of *Yersinia*-mediated inflammasome activation and evasion in human cells, and reveal species-specific differences underlying regulation of inflammasome responses to *Yersinia*.

Importance *Yersinia* are responsible for significant disease burdens in humans, ranging from recurrent disease outbreaks (yersiniosis) to pandemics (*Yersinia pestis* plague). Together with rising antibiotic resistance rates, there is a critical need to better understand *Yersinia* pathogenesis and host immune mechanisms, as this information will aid in developing improved immunomodulatory therapeutics. Inflammasome responses in human cells are less studied relative to murine models of infection, though recent studies have uncovered key differences in inflammasome responses between mice and humans. Here, we dissect human intestinal epithelial cell and macrophage inflammasome responses to *Yersinia pseudotuberculosis.* Our findings provide insight into species- and cell type-specific differences in inflammasome responses to *Yersinia.*

Introduction

Innate immunity is a critical component of host defense and employs pattern recognition receptors (PRRs) to detect pathogen-associated molecular patterns (PAMPs) (1, 2). Specific cytosolic PRRs in the Nucleotide-binding domain and Leucine-rich Repeat-containing protein (NLR) family induce the formation and activation of multimeric immune complexes known as inflammasomes in response to cytosolic PAMPs and virulence-associated activities (3–5). The NLRP3 inflammasome is activated by a variety of stimuli, including potassium efflux

54 downstream of bacterial-induced pore formation (5–9), whereas the NAIP-NLRC4
55 inflammasome responds to bacterial flagellin and components of bacterial type III secretion
56 systems (T3SS) (10–18). Inflammasomes recruit and activate caspase-1, which in turn
57 processes members of the IL-1 family of cytokines and the pore-forming protein GSDMD into
58 their active forms (19–23). In addition to these canonical inflammasome pathways, a non-
59 canonical caspase-4 inflammasome in humans, and orthologous caspase-11 inflammasome in
60 mice, responds to cytosolic lipopolysaccharide (LPS) during gram-negative bacterial infection to
61 initiate GSDMD processing, pore formation, and cytokine release (24–31). Consequently,
62 inflammasome activation leads to release of active IL-1 family cytokines, specifically IL-1β and
63 IL-18, and an inflammatory form of cell death known as pyroptosis, that collectively amplify
64 immune signaling and promote anti-bacterial defense (32). In parallel, bacterial infection triggers
65 other programmed cell death pathways, including apoptosis and necroptosis, thereby providing
66 multiple layers of defense against bacterial pathogens (33, 34).
67 The enteric pathogenic Yersiniae, *Yersinia pseudotuberculosis* and *Y. enterocolitica,*
68 express a conserved T3SS that injects *Yersinia* outer proteins (Yops) into target cells (35).
69 T3SS-injected Yops manipulate host cellular pathways to promote infection, but also activate
70 and inhibit effector-triggered cell death responses. For example, in murine macrophages, YopJ-
71 mediated suppression of NF-κB signaling induces apoptosis, whereas YopE-mediated
72 disruption of cytoskeletal dynamics activates the pyrin inflammasome and hyper-translocation of
73 T3SS components in the absence of YopK activates the NLRP3 and caspase-11
74 inflammasomes (36–45). Notably, *Yersinia* utilizes two other effectors, YopM and YopK, to
75 evade YopE-triggered pyrin and T3SS-triggered NLRP3/caspase-11-inflammasome activation
76 respectively and promote infection (42, 43, 45, 46). Collectively, these virulence strategies
77 manipulate the host in order to facilitate colonization and evade ensuing effector-triggered
78 immunity (47).
79 Inflammasome responses to *Yersinia* have primarily been studied in murine
80 macrophages. However, fundamental differences exist between human and murine
81 inflammasome responses to bacterial infection that may impact pathogenesis and disease
82 severity in the host, including ligand recognition, virulence-driven immune suppression, and
83 inflammasome component expression (48–68). Furthermore, beyond phagocytic cells,
84 inflammasomes are expressed in multiple cell types, including intestinal epithelial cells (IECs)
85 (69), which are a primary site of infection and interact significantly with enteric pathogens during
86 intestinal colonization. While specialized IECs known as M cells, which overlie intestinal immune
87 compartments called Peyer's patches, are considered the primary point of bacterial invasion of

88 the intestinal epithelial barrier (70)(71)(72)(73), *Yersinia* microcolonies are frequently found
89 outside of Peyer's patches within submucosal pyogranulomas and in close proximity to non-M
90 cell IECs (74). Importantly, many enteric bacterial pathogens use secreted virulence factors to
91 inhibit IEC death in order to preserve their replicative niche during early infection (75, 76). *Y.*
92 *enterocolitica* uses two anti-phagocytic Yops, YopE and YopH, to evade caspase-1 and NLRP3-
93 dependent inflammasome activation in human IECs (77). However, the role of other Yops or
94 other inflammasomes in IECs and human cells broadly is unknown.
95 Here, we find that in contrast to prior findings in murine macrophages (38, 44, 78, 79),
96 the *Y. pseudotuberculosis* (*Yptb*) effector YopJ does not induce death of human IECs or
97 macrophages. In contrast, in human cells, *Yptb* evades caspase-4- and GSDMD-dependent cell
98 death and inflammasome-dependent cytokine release. Notably, the type III secreted effectors
99 YopE, YopH, and YopK, collectively enable *Yptb* to evade caspase-4 activation in human cells.
100 Mechanistically, YopE and YopH blockade of bacterial internalization prevented accumulation of
101 intracellular bacteria and correlated with reduced inflammasome activation. Furthermore, the
102 *Yptb* adhesin YadA and host β1-integrins were required for *Yptb* internalization into human IECs
103 and subsequent caspase-4 activation in the absence of YopE, YopH, and YopK. These findings
104 demonstrate a key role for disruption of actin-mediated internalization in *Yersinia* evasion of the
105 noncanonical inflammasome in human IECs, and uncover important species and cell-type-
106 specific differences in inflammasome responses to *Yersinia* infection.
107
108 **Results**
109 ***Yptb* effectors evade T3SS-dependent inflammasome activation in human cells**
110 During infection of murine macrophages, *Yersinia* injects Yops to evade inflammasome
111 activation (42, 43, 45, 46). However, wild type (WT) *Yersinia* induces rapid cell death (Fig. 1A)
112 and caspase-8 and caspase-1 activation due to YopJ-mediated inhibition of NF-κB and MAPK
113 signaling, enabling antibacterial defense despite effector-mediated immune modulation (38, 44,
114 78, 79). In contrast, human macrophages and IECs do not undergo YopJ-dependent cell death
115 early during *Y. enterocolitica* infection or at all during *Y. pseudotuberculosis* infection (56, 77,
116 80). In agreement with these findings, infection of the human colorectal cell line Caco-2 (Fig.
117 1B) or primary human monocyte-derived macrophages (hMDMs) (Fig. 1C) with WT *Yptb* failed
118 to induce release of lactate dehydrogenase (LDH), a marker of cell lysis, into the supernatant.
119 Furthermore, WT *Yptb* infection of the human monocytic cell line THP-1 macrophages similarly
120 failed to induce LDH release (Fig. S1A), collectively suggesting that in contrast to murine cells,
121 human cells do not undergo cell death in response to WT *Yptb* infection.

122 Lack of cell death in *Yptb*-infected human cells could be due to a failure to initiate
123 programmed cell death pathways, or due to active evasion or suppression of programmed cell
124 death by the bacteria. *Y. enterocolitica* deploys two injected effectors, YopH and YopE, to evade
125 inflammasome activation in human IECs (77). Critically, *Yptb* lacking all six of its injected
126 effectors *(*Δ*6 Yptb*) triggered significantly higher levels of cell death compared to either mock or
127 WT *Yptb*-infected cells in Caco-2 IECs (Fig. 1B), hMDMs (Fig. 1C) and THP-1 macrophages
128 (Fig. S1A). Further, Δ*6 Yptb*-infected polarized and non-polarized Caco-2 cells robustly cleaved
129 and released the inflammasome-dependent cytokine IL-18 compared to mock or WT *Yptb*-
130 infected cells (Fig. S1B, Fig. 1D-E). IL-18 release following Δ*6 Yptb* infection occurred at a
131 range of increasing doses, whereas WT *Yptb* failed to induce IL-18 release even at the highest
132 doses (Fig. S1C). Consistent with our and others' findings that expression and release of the
133 inflammasome-dependent cytokine IL-1β is very low in human IECs (48, 49, 77), we did not
134 detect IL-1β release during Δ*6 Yptb* infection (Fig. S1D). While IECs do not produce IL-1β, this
135 cytokine is released by macrophages undergoing pyroptosis. Indeed, hMDMs and THP-1
136 macrophages infected with Δ*6 Yptb* robustly cleaved and secreted IL-1β in contrast to mock or
137 WT *Yptb*-infected cells (Fig. 1F-G, Fig. S1E), collectively indicating that in the absence of its
138 injected effectors, *Yersinia* triggers inflammasome activation in multiple human cell types. As
139 expected, inflammasome activation in response to Δ*6 Yptb* infection is T3SS-dependent, as an
140 isogenic *Yptb* strain cured of its virulence plasmid encoding the T3SS did not induce IL-18
141 release in human IECs (Fig. 1D). Collectively, these results indicate that Yops enable WT *Yptb*
142 to evade inflammasome activation in human cells, a fundamentally distinct outcome from the
143 induction of apoptosis and pyroptosis triggered in murine macrophages by WT *Yersinia* (38, 44,
144 78, 79).
145
146 **Caspase-4 is required for Δ*6 Yptb*-induced inflammasome activation in human cells**
147 Caspases play important roles in cleaving and activating inflammasome-dependent
148 cytokines and executing cell death (34). Pretreatment of Caco-2 cells with the pan-caspase
149 inhibitor ZVAD prior to infection with Δ*6 Yptb* completely abrogated IL-18 release and cell death
150 compared to the vehicle control (Fig. 2A-B), indicating that caspases mediate inflammasome
151 activation downstream of Δ*6 Yptb* infection in human IECs. As ZVAD broadly inhibits multiple
152 caspases, we next sought to determine which specific caspases are required for Δ*6 Yptb*-
153 induced inflammasome activation in human IECs. Caspase-1 is critical for inflammasome-
154 dependent cytokine release and pyroptosis during bacterial infection (34, 44, 64, 81), and is
155 activated during *Y. enterocolitica* infection of Caco-2 cells (77). Δ*6 Yptb* infection of two

156 independent clones of *CASP1*$^{-/-}$ Caco-2 cells (49) resulted in a partial loss of IL-18 release
157 compared to WT Caco-2 cells (Fig. S2A). Similarly, WT Caco-2s pretreated with the caspase-1
158 inhibitor YVAD exhibited incomplete loss of IL-18 release after Δ*6 Yptb* infection compared to
159 DMSO vehicle-treated cells (Fig. S2B), suggesting that caspase-1 contributes to, but is not
160 absolutely required for, Δ*6 Yptb*-induced inflammasome activation. Caspase-8 is activated in
161 murine macrophages and IECs in response to infection by multiple pathogens, including
162 *Yersinia* (44, 82, 83), and can process caspase-1 substrates such as IL-1β and GSDMD to
163 mediate pyroptosis in the absence of caspase-1 (64, 82, 84). Notably, siRNA knockdown of
164 *CASP8* and pretreatment with the caspase-8 inhibitor IETD resulted in a partial reduction in IL-
165 18 release following Δ*6 Yptb* infection (Fig. S2C-E), suggesting that like caspase-1, caspase-8
166 partially contributes to inflammasome activation during Δ*6 Yptb* infection. However, *CASP8*
167 siRNA knockdown in *CASP1*$^{-/-}$ Caco-2 cells did not abrogate inflammasome activation during Δ*6*
168 *Yptb* infection (Fig. S2F-G), indicating that additional caspase activation pathways likely mediate
169 cell death during Δ*6 Yptb* infection of human IECs.
170 Caspase-4 plays a critical role in inflammasome responses to a variety of enteric
171 pathogens in human IECs (48, 49, 60, 67), and its activation triggers both IEC death and IL-18
172 release (48). To test whether caspase-4 contributes to inflammasome responses to Δ*6 Yptb*, we
173 infected two independent single-cell clones of *CASP4*$^{-/-}$ Caco-2 cells (49) with either WT or Δ*6*
174 *Yptb*. As expected, WT *Yptb* infection did not elicit inflammasome activation in either WT or
175 *CASP4*$^{-/-}$ Caco-2 cells, and Δ*6 Yptb* infection of WT Caco-2 cells resulted in robust release of
176 cleaved IL-18 and cell death. Notably, *CASP4* deficiency abrogated cleavage and release of
177 active IL-18 and cell death in response to Δ*6 Yptb*, indicating that caspase-4 is absolutely
178 required for inflammasome responses to Δ*6 Yptb* infection in human IECs (Fig. 2C-E). Further,
179 *CASP4* deficiency in THP-1 macrophages (85) resulted in a partial but significant decrease in
180 inflammasome activation (Fig. S3A), suggesting that Yop-mediated evasion of the caspase-4
181 inflammasome is a conserved evasion mechanism across human cell types. Loss of
182 inflammasome activation in THP-1 macrophages lacking caspase-4 largely mirrored our findings
183 with pretreatment with the pan-caspase inhibitor ZVAD (Fig. S3B), further supporting caspase-4
184 contribution to inflammasome activation in human macrophages. Caspase-5 contributes to
185 *Salmonella*-induced inflammasome activation in Caco-2 cells (49). To test whether caspase-5
186 also contributes to Δ*6 Yptb*-induced inflammasome activation in Caco-2 cells, we treated WT
187 Caco-2 cells with either a control scramble siRNA or *CASP5* siRNA. Knockdown of *CASP5*
188 resulted in a partial decrease in IL-18 release (Fig. S3C and S3D), suggesting that caspase-5
189 contributes but is not absolutely required for inflammasome activation. Collectively, these data

190 indicate for the first time that *Yptb* deploys its Yops to evade caspase-4 inflammasome
191 activation in human macrophages and IECs.
192
193 **GSDMD is required for Δ*6 Yptb*-induced inflammasome-dependent cytokine release and**
194 **cell death in human cells**
195 Inflammasome activation leads to cleavage of the protein GSDMD and liberation of its
196 active pore-forming N-terminal domain, leading to its oligomerization into a large ungated pore
197 (19, 25, 86). Formation of the GSDMD pore in the plasma membrane leads to release of IL-1
198 family cytokines as well as cell lysis and death, collectively termed "pyroptosis" (87–90).
199 Caspase-4 cleaves and activates GSDMD via release of its N-terminal domain (25, 91).
200 Notably, Δ*6 Yptb* infection led to robust GSDMD cleavage in WT Caco-2 cells, which was
201 completely absent in *CASP4*$^{-/-}$ Caco-2 cells, indicating that caspase-4 is required for GSDMD
202 cleavage in human IECs in response to *Yersinia* lacking its secreted effectors (Fig. 3A). In
203 contrast, consistent with a lack of observed cell death and IL-18 release, WT *Yptb* infection did
204 not elicit GSDMD cleavage in either WT or *CASP4*$^{-/-}$ IECs (Fig. 3A). To test whether GSDMD is
205 required for cell death and inflammasome-dependent cytokine release during Δ*6 Yptb* infection,
206 we pretreated Caco-2 cells with disulfiram, a chemical inhibitor of GSDMD pore formation (92).
207 Critically, disulfiram treatment completely abrogated IL-18 release and cell death downstream of
208 inflammasome activation in Δ*6 Yptb*-infected cells compared to infected vehicle control treated
209 cells (Fig. 3B-C). Consistent with this observation in human IECs, disulfiram treatment of human
210 THP-1 macrophages resulted in an abrogation of IL-1β release (Fig. 3D). Collectively, these
211 results indicate that *Yptb* Yops enable evasion of the caspase-4 inflammasome and GSDMD
212 activation.
213 The NLRP3 inflammasome can be activated by a variety of stimuli during infection,
214 including potassium efflux downstream of caspase-4-dependent GSDMD activation and pore
215 formation (5–9). Previous studies of human IEC responses during *Y. enterocolitica* infection
216 identified a critical role for the NLRP3 inflammasome (77). However, studies of human IECs
217 found that NLRP3 does not play a role in inflammasome activation in response to *Salmonella*
218 infection, potentially due to very low levels of NLRP3 expression in human IECs as compared to
219 human macrophages (49, 93, 94). In agreement, WT Caco-2 cells pretreated with a chemical
220 inhibitor of the NLRP3 inflammasome, MCC950, underwent comparable levels of inflammasome
221 activation in response to Δ*6 Yptb* infection as infected vehicle control-treated Caco-2 cells (Fig.
222 S4A). Caco-2 cells stimulated with LPS and nigericin, a known agonist of the NLRP3
223 inflammasome, also failed to induce IL-18 release, further suggesting a lack of NLRP3

224 inflammasome activity in Caco-2 cells. The NAIP/NLRC4 inflammasome, which senses and
225 responds to flagellin and T3SS ligands (10–18) (Fig. S4B), and the inflammasome adaptor
226 protein ASC (Fig. S4C) were also dispensable for Δ*6 Yptb*-induced inflammasome activation,
227 consistent with prior findings that expression of these proteins is very low in human IECs (49).
228 Collectively, these results indicate that the canonical NLRP3 and NAIP/NLRC4 inflammasomes,
229 as well as broadly ASC-dependent inflammasomes, are not activated during Δ*6 Yptb* infection
230 of Caco2 cells, and that GSDMD cleavage and activation occurs downstream of caspase-4 and
231 is required for cell death and cytokine release.
232
233 **YopE, YopH, and YopK synergistically enable *Yptb* to evade human inflammasome**
234 **responses**
235 Our findings demonstrate that *Yptb* lacking its entire repertoire of injected effectors
236 induce inflammasome activation in human IECs (Fig. 1). In contrast, Caco-2 cells infected with a
237 panel of *Yptb* mutant strains each lacking one of the six Yops failed to elicit IL-18 secretion (Fig.
238 4A), indicating that loss of any single secreted Yop was insufficient to alleviate inflammasome
239 evasion and that several Yops likely have overlapping functions in evading inflammasome
240 activation. Notably, single loss of YopK and YopM failed to induce inflammasome activation
241 (Fig. 4A), despite their roles in evading the NLRP3/caspase-11 and pyrin inflammasomes
242 respectively in murine macrophages (40, 43, 45, 46). *Y. enterocolitica* was previously reported
243 to regulate NLRP3 inflammasome activation in Caco-2 cells by a combination of YopE and
244 YopH-mediated blockade of integrin signaling (77). Despite a lack of a role for the NLRP3
245 inflammasome during Δ*6 Yptb* infection of human IECs (Fig. S4A), *Yptb* lacking both YopE and
246 YopH *(*Δ*yopEH Yptb*) elicited significantly elevated IL-18 release in Caco-2 cells, indicating that
247 combinatorial loss of both YopE and YopH was sufficient to induce inflammasome activation in
248 human IECs (Fig. 4B). Nonetheless, IL-18 levels during Δ*yopEH Yptb* infection were
249 significantly lower than IL-18 levels released during Δ*6 Yptb* infection (Fig. 4B), suggesting that
250 additional Yops contribute to inflammasome evasion during *Yersinia* infection of human IECs.
251 YopK is a translocated effector that negatively regulates the translocation of other Yops
252 and T3SS components (42, 43, 45). In murine macrophages, YopK evades inflammasome
253 activation, whereas YopE and YopH do not contribute to inflammasome evasion (42, 43, 45).
254 Given that deletion of *yopK* alone failed to elicit IL-18 release in human IECs (77) (Fig. 4A), we
255 considered that YopK could modulate inflammasome activation in human IECs in a manner that
256 is masked by YopE and YopH, perhaps because these effectors are hypertranslocated in a
257 Δ*yopK* mutant. Indeed, IL-18 release during Δ*yopEHK Yptb* infection was substantially elevated

258 compared to Δ*yopEH Yptb,* and fully recapitulated levels of IL-18 release observed during Δ*6*
259 *Yptb* infection (Fig. 4B), indicating that YopE, YopH and YopK function together to enable *Yptb*
260 evasion of inflammasome activation during infection. Critically, individual loss of YopK, dual loss
261 of YopK and YopE *(*Δ*yopEK*) or dual loss of YopK and YopH *(*Δ*yopHK*) all failed to induce
262 inflammasome activation. Only in a *yopEH* mutant background did additional deletion of YopK
263 lead to an increase in IL-18 release (Fig. 4B). Consistent with infection of human IECs,
264 Δ*yopEHK* infection also triggered higher levels of inflammasome activation than either Δ*yopEH*
265 or Δ*yopK* infection in human THP-1 macrophages (Fig. 4C-D). Further, as with Δ*6 Yptb*
266 infection, Δ*yopEHK*-induced inflammasome activation in Caco-2 cells was fully dependent on
267 caspase-4 (Fig. 4E-F). Taken together, these data suggest that YopE, YopH, and YopK act in
268 concert to evade the noncanonical inflammasome in both human IECs and macrophages.
269 These results are distinct from murine macrophages, in which YopE instead activates the pyrin
270 inflammasome, and YopK and YopM contribute to inflammasome evasion (42, 43, 45, 46).
271
272 **YopE and YopH inhibit caspase-4-dependent inflammasome activation in human IECs by**
273 **blocking actin-dependent bacterial internalization**
274 During *Y. enterocolitica* infection of human IECs, YopE and YopH evade NLRP3
275 inflammasome activation by disrupting IL-18 transcriptional priming downstream of invasin-β1-
276 integrin signaling (77). However, *Yersinia* adhesin-β1-integrin-mediated signaling also triggers
277 host cytoskeletal rearrangements to facilitate bacterial internalization (95–98). YopE and YopH
278 disruption of focal adhesion complexes and actin filamentation consequently inhibits *Yersinia*
279 uptake into host cells (98–108). Notably, consistent with both Δ*6* and Δ*yopEHK Yptb* infection,
280 we found that caspase-4 was absolutely required for inflammasome activation induced by
281 Δ*yopEH Yptb* (Fig. 5A and 5B). Considering YopE and YopH's known roles in inhibiting
282 bacterial internalization, we hypothesized that YopE- and YopH-mediated inflammasome
283 evasion in human IECs might be linked to their antiphagocytic activity, which would limit
284 bacterial internalization, subsequent cytosolic delivery of LPS, and caspase-4 inflammasome
285 activation. Consistent with previous reports (98, 100–102, 104, 108), levels of *Yptb*
286 internalization into human cells 2 hours post-infection were lowest in WT *Yptb*-infected cells,
287 while Δ*yopEH*-infected cells had significantly elevated levels of intracellular bacteria, as
288 assessed by colony forming units (CFUs) (Fig. S5A-B). Δ*yopEH* and Δ*6*-infected cells had
289 comparable levels of intracellular bacteria at 2 hpi, indicating that YopE and YopH regulate
290 internalization into human cells, while YopK limits inflammasome activation through a
291 mechanism distinct from bacterial internalization. In agreement with our CFU data, microscopic

292 analysis of Caco-2 cells infected with GFP-expressing bacteria demonstrated that Δ*yopEH* and
293 Δ*6 Yptb*-infected cells had significantly higher levels of intracellular bacteria (i.e. GFP-only
294 bacteria) than WT *Yptb*-infected cells (Fig. S5C-D). Furthermore, coinfection of Caco-2 cells
295 with Δ*6 Yptb* and increasing doses of WT *Yptb* resulted in reduced bacterial internalization (Fig.
296 5C), which corresponded to a dose-dependent decrease in inflammasome activation (Fig. 5D)
297 as compared to Δ*6 Yptb* alone infected cells. These results suggest that WT *Yptb*-injected Yops
298 act in trans and can complement inhibition of bacterial uptake and inflammasome activation
299 during Δ*6 Yptb* infection. As YopE and YopH block bacterial uptake via disruption of the actin
300 cytoskeleton (98, 101–107), we asked whether pharmacological inhibition of the actin
301 cytoskeleton would prevent inflammasome activation in response to Δ*yopEH Yptb* infection.
302 Notably, cytochalasin D, an inhibitor of actin polymerization previously demonstrated to block
303 bacterial internalization (102, 109), significantly reduced both intracellular bacterial numbers and
304 inflammasome activation during Δ*yopEH* infection (Fig. S5E-F). Collectively, these results
305 highlight a role for YopE and YopH-mediated internalization inhibition in contributing to
306 inflammasome evasion in human IECs.
307
308 **YadA and β1-integrin are necessary for bacterial internalization and inflammasome**
309 **activation**
310 Because Cytochalasin D has pleiotropic inhibitory effects, we sought to evaluate the role
311 of bacterial internalization in triggering inflammasome activation by manipulating components of
312 β1-integrin signaling. As macrophages are naturally phagocytic and do not require β1-integrin
313 signaling to induce bacterial uptake, we focused on human IECs. *Yersinia*-β1-integrin
314 interactions initiate an intracellular signaling cascade, including phosphorylation of the
315 serine/threonine kinase Akt, that ultimately regulates actin-dependent cellular changes
316 necessary for bacterial internalization (110–115). Consistent with previous reports, chemical
317 inhibition of Akt isoforms 1 and 2 diminished Δ*6 Yptb* internalization in IECs (Fig. S6A) (116).
318 Critically, inflammasome activation induced by Δ*6 Yptb* was also significantly blunted in the
319 presence of Akt inhibitors (Fig. S6B). Further, pretreatment with an anti-β1-integrin blocking
320 antibody previously found to reduce *Yersinia* entry into cells (117), also significantly decreased
321 bacterial internalization and inflammasome activation during both Δ*yopEH* and Δ*6 Yptb* infection
322 (Fig. 5E-F). Moreover, siRNA knockdown of α5β1 integrin similarly reduced levels of
323 internalized bacteria and inflammasome activation (Fig. S6C-E). Together, these data suggest
324 that disruption of β1-integrin receptor engagement and downstream components of β1-integrin
325 signaling prevents *Yersinia* internalization and limits inflammasome activation in IECs.

326 The *Yersinia* adhesin, invasin, binds to β1-integrin to facilitate efficient bacterial
327 internalization into mammalian cells, particularly during early intestinal invasion and
328 translocation through M cells (70, 118). Inflammasome activation during *Y. enterocolitica*
329 infection of human IECs was found to be dependent on invasin-β1-integrin signaling that
330 upregulates *Il18* transcript levels (77). However, unlike *Ye, Yptb* does not express high levels of
331 invasin under T3SS-expressing conditions (117, 119, 120). Consistently, deletion of invasin had
332 a minor impact on Δ*yopEH* and Δ*6 Yptb*-induced internalization and inflammasome activation
333 (Fig. S6F-G) suggesting the possibility that other adhesins may mediate T3SS-dependent
334 inflammasome activation by *Yptb*. YadA is encoded on the *Yersinia* virulence plasmid, and its
335 expression is co-regulated with the T3SS and Yops (121). As YadA mediates efficient cellular
336 entry under conditions where invasin expression is repressed (117), we hypothesized that
337 YadA-mediated bacterial internalization might drive caspase-4-dependent inflammasome
338 activation. Indeed, deletion of YadA in both Δ*yopEH* and Δ*6 Yptb* significantly reduced bacterial
339 internalization to levels comparable to WT infection (Fig. 5G) and completely abrogated
340 inflammasome activation (Fig. 5H). Notably, deletion of YadA alone largely phenocopied
341 deletion of both invasin and YadA with respect to internalization and inflammasome activation
342 (Fig. 5G-H), implicating YadA as the primary adhesin responsible for bacterial internalization
343 and inflammasome activation during *Yptb* infection of human IECs.
344
345 **Discussion**
346 In this study, we report for the first time that the *Yptb* T3SS-injected effectors YopE,
347 YopH and YopK collectively enable evasion of caspase-4 inflammasome activation and
348 pyroptosis in human cells (Fig. 1-4, S1, S3). Mechanistically, YopE and YopH prevented
349 bacterial internalization and, together with YopK, limited caspase-4 inflammasome activation
350 downstream of YadA-β1-integrin-mediated uptake of *Yptb* into IECs (Fig. 5, S5-6).
351 The NLRP3 inflammasome is reported to be activated by *Y. enterocolitica* in human
352 IECs (77). However, we found that NLRP3 was dispensable for inflammasome responses to
353 *Yptb* in Caco-2 cells (Fig. S4A). NLRP3 expression is very low in Caco-2 IECs and primary
354 human epithelium (49, 93, 94), and other enteric pathogens and known NLRP3 stimuli fail to
355 activate the NLRP3 inflammasome in Caco-2 cells (49) (Fig. S4A). Differences in cell culture
356 conditions or between *Y. enterocolitica* and *Y. pseudotuberculosis* may account for the
357 differential role of NLRP3 during infection of human IECs. Moreover, the adaptor protein ASC,
358 which is necessary for function of the NLRP3, pyrin, and other inflammasomes, was
359 dispensable for inflammasome responses to Δ*6 Yptb* (Fig. S4C), indicating that canonical

360 inflammasomes are unlikely to be involved in this response. Notably, although YopE-mediated
361 cytoskeletal disruption activates the pyrin inflammasome, which is inhibited by YopM during
362 infection of murine macrophages (40, 46), YopM had no impact on inflammasome activation in
363 human IECs even in the presence of YopE (Fig. 4A), potentially due in part to low expression of
364 pyrin in IECs (122, 123).
365 We found instead for the first time that *Yptb* activates the caspase-4 inflammasome in
366 human epithelial cells (Fig. 2C-E, 4E-F, 5A-B). Caspase-4 is more highly expressed in human
367 IECs than other inflammasome components (49), and a broad range of intracellular enteric
368 pathogens engage or inhibit caspase-4/11 in human and murine IECs (48, 49, 76, 60, 62–67,
369 75). We also found a partial role for caspase-1 and caspase-8 in inflammasome activation in
370 Caco-2 cells (Fig. S2A-B, S2D-E). Caspase-8 and caspase-1 can be recruited to the same
371 inflammasome complexes and have compensatory or sequential roles (44, 64, 81).
372 Simultaneous knockdown of caspase-1 and caspase-8 still allowed for release of IL-18 during
373 Δ*6 Yptb* infection (Fig. S2F), suggesting that they are unlikely to play overlapping roles and may
374 act sequentially. Whether caspase-8 and capase-1 are activated downstream of caspase-4 or
375 are acting in a parallel pathway during *Yersinia* infection of human IECs is unknown. CASP4$^{-/-}$
376 THP-1 macrophages also had reduced levels of inflammasome activation during Δ*6 Yptb*
377 infection (Fig S3A-B), suggesting that like in human IECs, caspase-4 contributes to Δ*6 Yptb*-
378 induced inflammasome activation in human macrophages.
379 In addition to blocking entry into epithelial cells (98, 101–104) (Fig. S5), YopE and H
380 also block bacterial internalization into M cells (77), specialized follicular epithelial cells overlying
381 Peyer's patches that are considered the primary site of entry across the intestinal epithelium for
382 *Yersinia* (70–73, 104). As such, invasin-dependent entry into M cells may occur prior to full
383 T3SS upregulation, thereby allowing the bacteria to cross the epithelium without triggering
384 inflammasome activation. Intriguingly, we found that Δ*6 Yptb* induces inflammasome activation
385 during both apical and basolateral infection of polarized Caco-2 cells, suggesting a role for non-
386 M cell IECs in inflammasome-mediated host defense. While integrins are predominantly
387 expressed apically on M cells and basolaterally on non-M cell IECs, intestinal pathogens can
388 interact with basolateral host receptors at cellular junctions either due to depolarization events
389 leading to apical receptor relocation or to focal discontinuities leading to luminal exposure of
390 basolateral elements (124–126). Furthermore, *Yptb* microcolonies are found outside Peyer's
391 patches within submucosal pyogranulomas in close proximity basolaterally to IECs (74). YopE
392 and YopH may prevent apical or basolateral uptake by non M-cell IECs that would otherwise
393 trigger inflammasome-mediated responses within the intestinal epithelium.

394 *Y. entercolitica* YopE and YopH were previously reported to inhibit inflammasome
395 activation by blocking a priming signal downstream of integrin signaling that upregulates *IL18*
396 transcript levels (77). However, integrin signaling is also crucial for bacterial internalization into
397 IECs. Using a variety of orthogonal approaches, we show here that disruption of integrin
398 signaling reduced inflammasome activation commensurate with reduced levels of *Yptb*
399 internalization by IECs (Fig. 5, S6). Additionally, YadA, rather than invasin, was required for *Δ6*
400 *Yptb*-induced inflammasome activation and bacterial internalization (Fig. 5G-H), consistent with
401 *Yptb* downregulation of invasin and YadA co-expression with the T3SS (117, 121). Our findings
402 lead us to propose a model in which YopE/H-dependent blockade of YadA-mediated bacterial
403 uptake by IECs limits delivery of LPS into the host cell, thereby allowing bacteria to evade the
404 noncanonical inflammasome. Because adhesin-integrin binding and signal transduction mediate
405 a variety of cellular outcomes, it is difficult to fully exclude the impact of additional factors on
406 inflammasome activation and evasion facilitated by YopE and YopH.
407 While YopE and YopH interfere with inflammasome responses during *Y. enterocolitica*
408 infection of human IECs, no role was previously found for the *Y. enterocolitica* homolog of
409 YopK, YopQ (77). Consistently, while loss of YopK alone had no effect on inflammasome
410 responses to *Yptb*, combinatorial loss of YopK, YopE, and YopH recapitulated the levels of
411 inflammasome activation observed with Δ*6 Yptb* infection, suggesting that YopK evades a
412 component of an inflammasome pathway masked by YopE and YopH (Fig. 4). In murine
413 macrophages, YopK prevents LPS-mediated inflammasome activation by preventing
414 destabilization of the *Yersinia*-containing vacuole (42, 43). In the absence of YopE, YopH, and
415 YopK, *Yersinia* may be more readily taken up and exposed to the host cell cytosol, potentially
416 due to vacuolar damage as a result of T3SS-mediated pore formation (42, 127). We found that
417 loss of YopK augments Δ*yopEH*-induced inflammasome activation in both human macrophages
418 and IECs, potentially pointing to a conserved mechanism by which YopK, E, and H enable *Yptb*
419 to evade inflammasome responses across human cell types. Further studies are needed to
420 determine precisely how the T3SS and YopK evade cytosolic *Yersinia* LPS exposure and
421 caspase-4 activation.
422 The synergistic evasion of the caspase-4 inflammasome by YopE, YopH, and YopK, as
423 well as the absence of YopJ-induced cell death, in both human IECs and THP-1 macrophages
424 is fundamentally distinct from the response to *Yptb* observed in murine macrophages. Human
425 cells may be intrinsically more resistant to pathogen-induced cell death due to altered
426 expression of prosurvival factors such as cellular FLICE-inhibitory protein (cFLIP) or A20.
427 Furthermore, unlike macrophages, IECs are not phagocytic, potentially allowing contamination

428 of the host cell cytosol by bacterial LPS to be a more specific indicator of virulence activity in
429 IECs and providing a rationale for increased reliance on caspase-4-mediated responses.
430 Further studies dissecting inflammasome responses between murine and human IECs and
431 macrophages will provide additional insight into cell type- and species-specific differences in the
432 mechanisms of inflammasome activation by bacterial pathogens.
433 Overall, our data demonstrate that Yops E, H, and K, enable *Yersinia*
434 *pseudotuberculosis* to evade caspase-4 inflammasome responses downstream of YadA-β1-
435 integrin signaling in human cells, thereby revealing a major difference in interactions between
436 Yops and inflammasomes in murine and human macrophages. Our study further highlights the
437 distinct nature of inflammasome responses and bacterial effector activities in different cell types
438 in mice and humans, which provides insight into how inflammasome responses and bacterial
439 virulence activities shape health and disease in mice and humans.
440
441
442
443
444
445

446 **Materials and Methods**

447

448 **Ethics statement**

449 All studies involving primary human monocyte-derived macrophages (hMDMs) were performed
450 in compliance with the requirements of the US Department of Health and Human Services and
451 the principles expressed in the Declaration of Helsinki. hMDMs from de-identified healthy
452 human donors were obtained from the University of Pennsylvania Human Immunology Core,
453 which holds Institutional Review Board approval. These samples are considered a secondary
454 use of de-identified human specimens and are exempt via Title 55 Part 46, Subpart A of 46.101
455 (b) of the Code of Federal Regulations.

456

457 **Bacterial strains and growth conditions**

458 *Yersinia* strains are described in Table S1 in the supplemental material. Δ*yopEHK*, Δ*yopEK*,
459 and Δ*yopHK* were generated by introducing a frameshift mutation of the *yopK* open reading
460 frame into the Δ*yopEH*, Δ*yopE* and Δ*yopH* backgrounds respectively using a plasmid provided
461 by Dr. James Bliska and an allelic exchange method (128). Δ*yopM* was generated by
462 introducing an unmarked deletion of the *yopM* open reading frame into IP2666 using a plasmid
463 provided by Dr. James Bliska and the same allelic exchange method. Δ*yopEH*Δ*inv* and Δ*6*Δ*inv*
464 strains were generated by introducing an unmarked deletion of the *invasin* open reading frame
465 into Δ*yopEH* and Δ*6* strains respectively using a plasmid provided by Dr. Joan Mecsas and the
466 same allelic exchange method. Δ*yopEH*Δ*yadA*, Δ*yopEH*Δ*inv*Δ*yadA*, Δ*6*Δ*yadA*, and
467 Δ*6*Δ*inv*Δ*yadA* strains were generated by introducing a kanamycin resistance cassette in place
468 of the *yadA* open reading frame into Δ*yopEH,* Δ*yopEH*Δ*inv,* Δ*6,* and Δ*6*Δ*inv* strains respectively
469 using a plasmid provided by Dr. Petra Dersch and the same allelic exchange method. Yersiniae
470 were cultured overnight at 26°C with aeration in 2x yeast extract-tryptone (YT) broth. To induce
471 T3SS expression, in the morning, the bacteria were diluted into fresh 2xYT containing 20 mM
472 sodium oxalate and 20 mM $MgCl_2$. Bacteria were grown with aeration for 1 hour at 26°C
473 followed by 2 hour at 37°C prior to infection. All cultures were pelleted at 6000 x *g* for 3 min and
474 resuspended in phosphate-buffered saline (PBS). Cells were infected at an MOI of 60 unless
475 otherwise indicated, centrifuged at 290 x *g* for 10 min and incubated at 37°C. At 1 hour post-
476 infection, epithelial cells were treated with 20 ng/ml or 100 ng/ml of gentamicin for 6 hour or 2
477 hour time points respectively and macrophages were treated with 100 ng/ml of gentamicin for all
478 time points. Infections proceeded at 37°C for the indicated length of time for each experiment. In
479 all experiments control cells were mock infected with PBS.

480 **Cell culture conditions**

481 All cells were grown at 37°C in a humidified incubator with 5% CO_2.

482 Cell culture of Caco-2 cells

483 Caco-2 cells (HTB-27; American Type Culture Collection) were maintained in Dulbecco's
484 modified Eagle's medium (DMEM) supplemented with 10% (vol/vol) heat-inactivated fetal
485 bovine serum (FBS), 100 IU/mL penicillin and 100 μg/mL streptomycin. One day prior to
486 infection, Caco-2 cells were incubated with 0.25% trypsin-EDTA (Gibco) diluted 1:1 with 1 x
487 PBS at 37°C for 15 min to dissociate cells. Trypsin was neutralized with serum-containing
488 medium. Cells were replated in medium without antibiotics in a 24-well plate at a density of 3 x
489 10^5 cells/well and unprimed prior to infection as we have not observed differential
490 inflammasome-dependent cytokine release in IECs during infection with priming (49). All Caco-2
491 knockout cell lines are described previously (49).

492 Cell culture of polarized Caco-2 cells

493 Polarized Caco-2 cells were grown on polycarbonate 3 μM pore size cell culture inserts
494 (Corning 3415) in a 24 well plate. Inserts were coated with collagen coating solution containing
495 30 μg/ml collagen, 10 μg/ml fibronectin and 10 μg/ml BSA in DMEM and incubated for 3 hours.
496 Caco-2 cells were then plated in growth medium containing Corning MITO+ serum extender
497 (Fisher Scientific CB-50006) on inverted (for basolateral infection) or noninverted (for apical
498 infection) inserts. After 24 hours, the growth medium was replaced with Corning enterocyte
499 differentiation medium (Fisher Scientific 355357) with MITO+ serum extender. The media was
500 replaced daily and following three days of incubation in differentiation media, the transepithelial
501 electrical resistance was measured using an Epithelial Volt/Ohm (TEER) Meter (World Precision
502 Instruments) to ensure that resistance was above 250 $\Omega.cm^2$ prior to infection. Infections were
503 administered on the apical or basolateral side of cells as indicated.

504 Cell culture of THP-1 monocyte derived macrophages

505 THP-1 macrophages (TIB-202; American Type Culture Collection) were maintained in RPMI
506 supplemented with 10% (vol/vol) heat-inactivated fetal bovine serum (FBS), 0.05 nM β-
507 mercaptoethanol, 100 IU/mL penicillin and 100 μg/mL streptomycin. Two days prior to infection,
508 THP-1 cells were replated in medium without antibiotics in a 48-well plate at a density of 2 x 10^5
509 cells/well and incubated with phorbol 12-myristate 13-acetate (PMA) for 24 hours to allow
510 differentiation into macrophages. Macrophages were primed with 100 ng/mL Pam3CSK4
511 (Invivogen) for 16 hours prior to bacterial infections in order to upregulate pro-IL-1β transcript
512 levels.

513 Cell culture of primary human monocyte-derived macrophages (hMDMs)
514 Purified human monocytes from de-identified healthy human donors were obtained from the
515 University of Pennsylvania Human Immunology Core. Monocytes were differentiated into
516 macrophages by culturing in RPMI supplemented with 10% (vol/vol) heat-inactivated FBS, 2
517 mM L-glutamine, 100 IU/mL penicillin, 100 μg/ml streptomycin, and 50 ng/ml recombinant
518 human M-CSF (Gemini Bio-Products) for 6 days. Two days prior to infection, adhered hMDMs
519 were replated in media with 25 ng/ml human M-CSF lacking antibiotics at $1x10^5$ cells/well in a
520 48 well plate. hMDMs were then primed with 100 ng/ml Pam3CSK4 (Invivogen) for 16 hours
521 prior to bacterial infection in order to upregulate pro-IL-1β transcript levels.
522 Cell culture of murine bone marrow derived macrophages (BMDMs)
523 Bone marrow cells were grown in RPMI containing L-cell supernatant, heat-inactivated FBS,
524 penicillin and streptomycin for 8 days. One day prior to infection, differentiated BMDMs were
525 replated into 24-well dishes in media lacking antibiotics at a density of 2×10^5 cells/well.
526
527 **ELISAs**
528 Supernatants harvested from infected cells were assayed using enzyme-linked immunosorbent
529 assay (ELISA) kits for human IL-18 (R&D Systems) and IL-1β (BD Biosciences).
530
531 **LDH cytotoxicity assays**
532 Supernatants harvested from infected cells were assayed for cytotoxicity by measuring loss of
533 cellular membrane integrity via lactate dehydrogenase (LDH) assay. LDH release was
534 quantified using an LDH Cytotoxicity Detection Kit (Clontech) according to the manufacturer's
535 instructions and normalized to mock-infected (min cytotoxicity) and 2% triton-treated cells (max
536 cytotoxicity)
537
538 **Immunoblot analysis**
539 Cells were replated and infected on serum-free medium to collect supernatant samples.
540 Supernatant samples were centrifuged at 200 x *g* to pellet any cell debris and treated with
541 trichloroacetic acid (TCA) (25 μL TCA per 500 μL supernatant) overnight at 4°C. The following
542 day, TCA-treated samples were centrifuged at max speed (15,871 x *g*) for 15 min at 4°C and
543 washed with ice-cold acetone. TCA-precipitated supernatant samples and cell lysates were
544 resuspended in 1 x SDS-PAGE sample buffer and boiled for 5 min. Samples were separated by
545 SDS-PAGE on a 12% (vol/vol) acrylamide gel and transferred to polyvinylidene difluoride
546 (PVDF) Immobilon-P membranes (Millipore). Primary antibodies specific for human IL-18 (MLB

547 International PM014), IL-1β (R&D Systems MAB201), β-actin (4967L; Cell Signaling) and
548 GSDMD (G7422 Sigma-Aldrich) and horseradish peroxidase (HRP)-conjugated secondary
549 antibodies anti-rabbit IgG (7074S; Cell Signaling) and anti-mouse IgG (7076S; Cell Signaling)
550 were used. Enhanced chemiluminescence (ECL) Western blotting substrate or SuperSignal
551 West Femto (Pierce Thermo Scientific) HRP substrate were used for detection.
552
553 **Inhibitor and antibody blocking experiments**
554 Cells were treated 1 h prior to infection at the indicated concentrations of the following inhibitors:
555 10 μM MCC950 (Sigma-Aldrich; PZ0280), 20 μM pan-caspase inhibitor Z-VAD(Ome)-FMK (SM
556 Biochemicals; SMFMK001), 20 μM caspase-1 inhibitor Ac-YVAD-cmk (Sigma-Aldrich;
557 SML0429), 30 μM disulfiram (Sigma), 10 μM cytochalasin D (Sigma), and 25 μM Akt inhibitor
558 VIII (EMD Millipore). Cells were treated 1 h prior to infection with a 1:50 dilution of monoclonal
559 antibody 1987 clone P4C10 (EMD Millipore) directed against β1 integrins.
560
561 **siRNA-mediated gene knockdown**
562 *CASP5* (S2417), *CASP8* (S2427), *ITGA5* (S7549) and two Silencer Select negative-control
563 siRNAs (Silencer Select negative control no. 1 and no. 2 siRNA) were purchased from Ambion
564 (Life Technologies). Three days before infection, 30 nM siRNA was transfected into Caco-2
565 cells using Lipofectamine RNAiMAX transfection reagent (Thermo Fisher Scientific) following
566 the manufacturer's protocol.
567
568 **Quantitative RT-PCR analysis**
569 RNA was isolated using the RNeasy Plus Mini Kit (Qiagen) following the manufacturer's
570 instructions. Cells were lysed in 350 μL RLT buffer with β-mercaptoethanol and centrifuged
571 through a QIAshredder spin column (Qiagen). cDNA was synthesized from isolated RNA using
572 SuperScript II Reverse Transcriptase (Invitrogen) following the manufacturer's instructions.
573 Quantitative PCR was conducted with the CFX96 real-time system from Bio-Rad using the
574 SsoFast EvaGreen Supermix with Low ROX (Bio-Rad). For analysis, mRNA levels of siRNA-
575 treated cells were normalized to housekeeping gene *HPRT* and control siRNA-treated cells
576 using the $2^{-\Delta\Delta CT}$ (cycle threshold) method to calculate knockdown efficiency (129). The following
577 primers were used:
578 *CASP5* forward: TTCAACACCACATAACGTGTCC
579 *CASP5* reverse: GTCAAGGTTGCTCGTTCTATGG
580 *CASP8* forward: GTTGTGTGGGGTAATGACAATCT

581 *Casp8* reverse: TCAAAGGTCGTGGTCAAAGCC
582 *ITGA5* forward: GGCTTCAACTTAGACGCGGAG
583 *ITGA5* reverse: TGGCTGGTATTAGCCTTGGGT
584 *HPRT* forward: CCTGGCGTCGTGATTAGTGAT
585 *HPRT* reverse: AGACGTTCAGTCCTGTCCATAA
586
587 **Bacterial uptake enumeration with colony forming units (CFUs)**
588 Cells were infected with indicated strains of *Yersinia* at an MOI of 20. 1 hpi, cells were treated
589 with 100 μg/mL of gentamicin to kill extracellular bacteria. 2 hpi the supernatants were aspirated
590 and cells were lysed with PBS containing 0.5% Triton to collect intracellular bacteria. Harvested
591 bacteria were serially diluted in PBS and plated on LB agar plates containing 2 μg/mL Irgasan.
592 Plates were incubated at 28°C for two days and CFUs were counted.
593
594 **Fluorescence microscopy of intracellular *Yersinia***
595 One day before infection 2 x 10^5 cells/well were plated on glass coverslips in a 24-well plate.
596 Cells were infected with indicated strains of *Yersinia* constitutively expressing GFP at an MOI of
597 20. At 2hpi, cells were washed 2 times with PBS, fixed with 4% paraformaldehyde for 10 min at
598 37°C and stored overnight at 4°C in PBS. The following day, cells were blocked for 30 min at
599 room temperature in blocking solution containing 1% BSA in PBS and incubated for 1 h at room
600 temperature in blocking solution with the polyclonal anti-*Yersinia* antibody SB349 diluted 1:1000
601 (kindly provided by Dr. James Bliska) (102). AF594-conjugated goat anti-Rabbit IgG antibody
602 (A-11012 Thermo Fisher Scientific) was diluted 1:500 in blocking solution was added to cells
603 and incubated for 45 min at room temperature. Cells were mounted on glass slides with DAPI
604 mounting medium (Sigma Fluoroshield). Coverslips were imaged on an inverted fluorescence
605 microscope (IX81; Olympus) and images were collected using a high-resolution charge-
606 coupled-devise camera (FAST1394; QImaging) at a magnification of 60x. Images were
607 analyzed and presented using SlideBook (version 5.0) software (Intelligent Imaging Innovations,
608 Inc.). %intracellular bacteria were scored in unblinded fashion by counting 20 captures per
609 coverslip for coverslips across independent triplicate experiments.
610
611 **Statistical analysis**
612 Prism 9.4.1 (GraphPad Software) was utilized for the graphing of data and all statistical
613 analyses. Statistical significance for experiments were determined using the appropriate test

614 and are indicated in each figure legend. Differences were considered statistically significant if
615 the *p* value was <0.05.
616
617 **Data availability**
618 All data are included in the manuscript and supplemental material. Bacterial strains available
619 upon request
620
621 **Acknowledgments**
622 We thank members of the Shin and Brodsky laboratories for helpful scientific
623 discussions. We thank Dr. James Bliska, Dr. Joan Mecsas, and Dr. Petra Dersch for generously
624 providing plasmids and Yop mutant strains.
625 We thank the Human Immunology Core of the Penn Center for AIDS Research and
626 Abramson Cancer Center for providing purified primary human monocytes.
627 This work is supported by NIH/NIAID grants AI151476, AI118861, AI123243 (S.S.),
628 AI128630, AI163596, and AI139102 (I.E.B). S.S. and I.E.B. are both recipients of the
629 Burroughs-Welcome Fund Investigators in the Pathogenesis of Infectious Disease Award. J.Z.
630 is a recipient of the NIH/NIAID Microbial Pathogenesis and Genomics training grant
631 5T32AI141393-03.
632
633

634 Figure 1. *Yptb* effectors evade T3SS-dependent inflammasome activation in human cells.
635 BMDMs (A), Caco-2 cells (B, D-E) or hMDMs (C, F-G) were infected with PBS (Mock), WT
636 *Yptb*, or Δ*6 Yptb*. (A-C) Cell death was measured as percent cytotoxicity normalized to cells
637 treated with 2% Triton at 6hpi. (D) Release of IL-18 into the supernatant was measured by
638 ELISA at 6hpi. (E) Lysates and supernatants collected 6hpi were immunoblotted for IL-18 and β-
639 actin. (F) Release of IL-1β into the supernatant was measured by ELISA at 6hpi. (G) Lysates
640 and supernatants collected 6hpi were immunoblotted for IL-1β and β-actin. ns — not significant,
641 * $p < 0.05$, ** $p < 0.01$ by t-test (A-C) or one-way ANOVA (D, F). Shown are averages and error
642 bars representing the standard deviation from at least three pooled experiments.
643
644 Figure 2. Caspase-4 is required for Δ*6 Yptb*-induced inflammasome activation in human cells.
645 (A, B) One hour prior to infection, WT Caco-2 cells were treated with 20 μM ZVAD or DMSO as
646 a vehicle control. Cells were then infected with PBS (Mock), WT *Yptb* or Δ*6 Yptb*. At 6hpi (A)
647 release of IL-18 into the supernatant was measured by ELISA and (B) cell death was measured
648 as percent cytotoxicity normalized to cells treated with 2% triton. (C-E) WT or two independent
649 single cell clones of *CASP4*$^{-/-}$ Caco-2 cells were infected with PBS (Mock), WT *Yptb* or Δ*6 Yptb*.
650 (C) Release of IL-18 into the supernatant was measured by ELISA at 6hpi. (D) Lysates and
651 supernatants collected 6hpi were immunoblotted for IL-18 and β-actin. (E) Cell death was
652 measured at 6hpi as percent cytotoxicity normalized to cells treated with 2% triton. ** $p < 0.01$,
653 **** $p < 0.0001$ by two-way ANOVA. Shown are averages and error bars representing the
654 standard deviation from at least three pooled experiments.
655
656 Figure 3. GSDMD is required for Δ*6 Yptb*-induced inflammasome-dependent cytokine release
657 and cell death in human cells. (A) WT or two independent single cell clones of *CASP4*$^{-/-}$ Caco-2
658 cells were infected with PBS (Mock), WT *Yptb* or Δ*6 Yptb*. Lysates and supernatants were
659 collected at 6hpi and immunoblotted for GSDMD and β-actin. One hour prior to infection, (B, C)
660 WT Caco-2 cells or (D) THP-1 macrophages were treated with 30 μM disulfiram or DMSO as a
661 vehicle control. Cells were then infected with PBS (Mock), WT *Yptb* or Δ*6 Yptb*. Release of (B)
662 IL-18 or (D) IL-1β into the supernatant and (C) percent cytotoxicity normalized to cells treated
663 with 2% triton were measured at 6hpi. ***$p<0.001$, **** $p < 0.0001$ by two-way ANOVA. Shown
664 are averages and error bars representing the standard deviation from at least three pooled
665 experiments.
666
667 Figure 4. YopE, YopH, and YopK synergistically enable *Yptb* to evade human inflammasome
668 responses. (A, B) WT Caco-2 cells or (C, D) WT THP-1 macrophages were infected with PBS
669 (Mock) or indicated strain of *Yptb*. Release of (A, B) IL-18 or (C) IL-1β into the supernatant and
670 (D) percent cytotoxicity normalized to cells treated with 2% triton was measured at 6hpi. (E, F)
671 WT or two independent single cell clones of *CASP4*$^{-/-}$ Caco-2 cells were infected with PBS
672 (Mock) or the indicated strain of *Yptb*. (E) Release of IL-18 into the supernatant and (F) percent
673 cytotoxicity normalized to cells treated with 2% triton were measured at 6hpi. * $p < 0.05$, ** $p <$
674 0.01, *** $p < 0.001$, **** $p < 0.0001$ by one-way ANOVA (A-D) or two-way ANOVA (E, F). Shown
675 are averages and error bars representing the standard deviation from at least three pooled
676 experiments.
677
678 Figure 5. YopE and YopH evade caspase-4-dependent inflammasome activation and actin-
679 dependent bacterial internalization in human IECs. (A, B) WT or two independent single cell
680 clones of *CASP4*$^{-/-}$ Caco-2 cells were infected with PBS (Mock) or the indicated strain of *Yptb*.
681 (A) Release of IL-18 into the supernatant and (B) percent cytotoxicity normalized to cells treated
682 with 2% triton were measured at 6hpi. (C, D) WT Caco-2 cells were infected with the indicated
683 MOI and strain of *Yptb*. (C) Cells were lysed at 2 hpi and bacteria were plated on *Yersinia*-

684 selective agar to calculate CFUs. (D) Release of IL-18 into the supernatant was measured at
685 6hpi. (E, F) WT Caco-2 cells were incubated for one hour with or without a 1:50 dilution of
686 antibody against β-1 integrin and then infected with PBS (Mock) or the indicated strain of *Yptb*
687 at an MOI of 20 (E) or 60 (F). (E) Cells were lysed at 2 hpi and bacteria were plated on *Yersinia*-
688 selective agar to calculate CFUs. (F) Release of IL-18 into the supernatant was measured at
689 6hpi. (G, H) WT Caco-2 cells were infected with PBS (Mock) or the strain of *Yptb* at an MOI of
690 20 (G) or 60 (H). (G) Cells were lysed at 2 hpi and bacteria were plated on *Yersinia*-selective
691 agar to calculate CFUs. (H) Release of IL-18 into the supernatant was measured at 6hpi. * $p <$
692 0.05, ** $p < 0.01$, *** $p < 0.001$, **** $p < 0.0001$ by two-way ANOVA (A, B) or one-way ANOVA
693 (C-H). Shown are averages and error bars representing the standard deviation from at least
694 three pooled experiments.
696

1. Janeway CA. 1989. Approaching the Asymptote? Evolution and Revolution in Immunology. Cold Spring Harb Symp Quant Biol 54:1–13.
2. Janeway CA, Medzhitov R. 2003. Innate Immune Recognition. https://doi.org/101146/annurev.immunol20083001084359 20:197–216.
3. Vance RE, Isberg RR, Portnoy DA. 2009. Patterns of Pathogenesis: Discrimination of Pathogenic and Nonpathogenic Microbes by the Innate Immune System. Cell Host Microbe 6:10–21.
4. Brodsky IE, Monack D. 2009. NLR-mediated control of inflammasome assembly in the host response against bacterial pathogens. Semin Immunol 21:199–207.
5. Lamkanfi M, Dixit VM. 2009. Inflammasomes: guardians of cytosolic sanctity. Immunol Rev 227:95–105.
6. Mariathasan S, Weiss DS, Newton K, McBride J, O'Rourke K, Roose-Girma M, Lee WP, Weinrauch Y, Monack DM, Dixit VM. 2006. Cryopyrin activates the inflammasome in response to toxins and ATP. Nat 2006 4407081 440:228–232.
7. Muñoz-Planillo R, Kuffa P, Martínez-Colón G, Smith BL, Rajendiran TM, Núñez G. 2013. K+ Efflux Is the Common Trigger of NLRP3 Inflammasome Activation by Bacterial Toxins and Particulate Matter. Immunity 38:1142–1153.
8. Hornung V, Bauernfeind F, Halle A, Samstad EO, Kono H, Rock KL, Fitzgerald KA, Latz E. 2008. Silica crystals and aluminum salts activate the NALP3 inflammasome through phagosomal destabilization. Nat Immunol 2008 98 9:847–856.
9. Franchi L, Kanneganti TD, Dubyak GR, Núñez G. 2007. Differential requirement of P2X7 receptor and intracellular K+ for caspase-1 activation induced by intracellular and extracellular bacteria. J Biol Chem 282:18810–18818.
10. Ren T, Zamboni DS, Roy CR, Dietrich WF, Vance RE. 2006. Flagellin-Deficient Legionella Mutants Evade Caspase-1- and Naip5-Mediated Macrophage Immunity. PLOS Pathog 2:e18.
11. Zhao Y, Yang J, Shi J, Gong Y-N, Lu Q, Xu H, Liu L, Shao F. 2011. The NLRC4 inflammasome receptors for bacterial flagellin and type III secretion apparatus https://doi.org/10.1038/nature10510.
12. Kofoed EM, Vance RE. 2011. Innate immune recognition of bacterial ligands by NAIPs determines inflammasome specificity https://doi.org/10.1038/nature10394.
13. Miao EA, Mao DP, Yudkovsky N, Bonneau R, Lorang CG, Warren SE, Leaf IA, Aderem A. Innate immune detection of the type III secretion apparatus through the NLRC4 inflammasome https://doi.org/10.1073/pnas.0913087107.
14. Zhao Y, Shi J, Shi X, Wang Y, Wang F, Shao F. 2016. Genetic functions of the NAIP family of inflammasome receptors for bacterial ligands in mice. J Exp Med 213:647–656.
15. Rauch I, Tenthorey JL, Nichols RD, Al Moussawi K, Kang JJ, Kang C, Kazmierczak BI, Vance RE. 2016. NAIP proteins are required for cytosolic detection of specific bacterial ligands in vivo. J Exp Med 213:657–665.
16. Yang J, Zhao Y, Shi J, Shao F. 2013. Human NAIP and mouse NAIP1 recognize bacterial type III secretion needle protein for inflammasome activation. Proc Natl Acad Sci U S A 110:14408–14413.
17. Rayamajhi M, Zak DE, Chavarria-Smith J, Vance RE, Miao EA. 2013. Cutting Edge: Mouse NAIP1 Detects the Type III Secretion System Needle Protein. J Immunol 191:3986–3989.
18. Molofsky AB, Byrne BG, Whitfield NN, Madigan CA, Fuse ET, Tateda K, Swanson MS. 2006. Cytosolic recognition of flagellin by mouse macrophages restricts Legionella pneumophila infection. J Exp Med 203:1093–1104.
19. Shi J, Zhao Y, Wang K, Shi X, Wang Y, Huang H, Zhuang Y, Cai T, Wang F, Shao F. 2015. Cleavage of GSDMD by inflammatory caspases determines pyroptotic cell death. Nat 2015 5267575 526:660–665.

20. Li P, Allen H, Banerjee S, Franklin S, Herzog L, Johnston C, Mcdowell J, Paskind M, Rodman L, Salfeld J, Towne E, Tracey D, Wardwell S, Wei F-Y, Wong W, Kamen R, Seshadri T. 1995. Mice Deficient in IL-lp-Converting Enzyme Are Defective in Production of Mature IL-lp and Resistant to Endotoxic Shock. Cell 80:401–411.
21. Kuida K, Lippke JA, Ku G, Harding MW, Livingston DJ, Su MSS, Flavell RA. 1995. Altered Cytokine Export and Apoptosis in Mice Deficient in Interleukin-1β Converting Enzyme. Science (80-) 267:2000–2003.
22. Cookson BT, Brennan MA. 2001. Pro-inflammatory programmed cell death [2]. Trends Microbiol 9:113–114.
23. Mariathasan S, Monack DM. 2007. Inflammasome adaptors and sensors: intracellular regulators of infection and inflammation. Nat Rev Immunol 2007 71 7:31–40.
24. Kayagaki N, Warming S, Lamkanfi M, Walle L Vande, Louie S, Dong J, Newton K, Qu Y, Liu J, Heldens S, Zhang J, Lee WP, Roose-Girma M, Dixit VM. 2011. Non-canonical inflammasome activation targets caspase-11. Nature 479:117–121.
25. Kayagaki N, Stowe IB, Lee BL, O'Rourke K, Anderson K, Warming S, Cuellar T, Haley B, Roose-Girma M, Phung QT, Liu PS, Lill JR, Li H, Wu J, Kummerfeld S, Zhang J, Lee WP, Snipas SJ, Salvesen GS, Morris LX, Fitzgerald L, Zhang Y, Bertram EM, Goodnow CC, Dixit VM. 2015. Caspase-11 cleaves gasdermin D for non-canonical inflammasome signalling. Nat 2015 5267575 526:666–671.
26. Rathinam VAK, Vanaja SK, Waggoner L, Sokolovska A, Becker C, Stuart LM, Leong JM, Fitzgerald KA. 2012. TRIF licenses caspase-11-dependent NLRP3 inflammasome activation by gram-negative bacteria. Cell 150:606–619.
27. Gurung P, Subbarao Malireddi RK, Anand PK, Demon D, Vande Walle L, Liu Z, Vogel P, Lamkanfi M, Kanneganti TD. 2012. Toll or interleukin-1 receptor (TIR) domain-containing adaptor inducing interferon-β (TRIF)-mediated caspase-11 protease production integrates toll-like receptor 4 (TLR4) protein- and Nlrp3 inflammasome-mediated host defense against enteropathogens. J Biol Chem 287:34474–34483.
28. Broz P, Ruby T, Belhocine K, Bouley DM, Kayagaki N, Dixit VM, Monack DM. 2012. Caspase-11 increases susceptibility to Salmonella infection in the absence of caspase-1. Nat 2012 4907419 490:288–291.
29. Kayagaki N, Wong MT, Stowe IB, Ramani SR, Gonzalez LC, Akashi-Takamura S, Miyake K, Zhang J, Lee WP, Muszyński A, Forsberg LS, Carlson RW, Dixit VM. 2013. Noncanonical inflammasome activation by intracellular LPS independent of TLR4. Science 341:1246–1249.
30. Shi J, Zhao Y, Wang Y, Gao W, Ding J, Li P, Hu L, Shao F. 2014. Inflammatory caspases are innate immune receptors for intracellular LPS. Nature 514:187–192.
31. Hagar JA, Powell DA, Aachoui Y, Ernst RK, Miao EA. 2013. Cytoplasmic LPS activates caspase-11: implications in TLR4-independent endotoxic shock. Science 341:1250–1253.
32. Lamkanfi M, Dixit VM. 2014. Mechanisms and Functions of Inflammasomes. Cell 157:1013–1022.
33. Lamkanfi M, Dixit VM. 2010. Manipulation of Host Cell Death Pathways during Microbial Infections. Cell Host Microbe 8:44–54.
34. Labbé K, Saleh M. 2008. Cell death in the host response to infection. Cell Death Differ 2008 159 15:1339–1349.
35. Cornelis GR, Wolf-Watz H. 1997. The Yersinia Yop virulon: a bacterial system for subverting eukaryotic cells. Mol Microbiol 23:861–867.
36. Bliska JB, Wang X, Viboud GI, Brodsky IE. 2013. Modulation of innate immune responses by Yersinia type III secretion system translocators and effectors. Cell Microbiol 15:1622–1631.
37. Viboud GI, Bliska JB. 2005. YERSINIA OUTER PROTEINS: Role in Modulation of Host

Cell Signaling Responses and Pathogenesis. https://doi.org/101146/annurev.micro59030804121320 59:69–89.

38. Palmer LE, Hobble S, Galán JE, Bliska JB. 1998. YopJ of Yersinia pseudotuberculosis is required for the inhibition of macrophage TNF-α production and downregulation of the MAP kinases p38 and JNK. Mol Microbiol 27:953–965.
39. Orth K, Palmer LE, Bao ZQ, Stewart S, Rudolph AE, Bliska JB, Dixon JE. 1999. Inhibition of the Mitogen-Activated Protein Kinase Kinase Superfamily by a Yersinia Effector. Science (80-) 285:1920–1923.
40. Medici NP, Rashid M, Bliska JB. 2019. Characterization of pyrin dephosphorylation and inflammasome activation in macrophages as triggered by the Yersinia effectors YopE and YopT. Infect Immun 87.
41. Wang X, Parashar K, Sitaram A, Bliska JB. 2014. The GAP Activity of Type III Effector YopE Triggers Killing of Yersinia in Macrophages. PLoS Pathog 10:1004346.
42. Zwack EE, Feeley EM, Burton AR, Baofeng H, Yamamoto M, Kanneganti T-D, Bliska JB, Coers J, Brodsky IE. 2017. Guanylate Binding Proteins Regulate Inflammasome Activation in Response to. Infect Immun 85:1–16.
43. Zwack EE, Snyder AG, Wynosky-Dolfi MA, Ruthel G, Philip NH, Marketon MM, Francis MS, Bliska JB, Brodsky IE. 2015. Inflammasome activation in response to the yersinia type III secretion system requires hyperinjection of translocon proteins YopB and YopD. MBio 6:1–11.
44. Philip NH, Dillon CP, Snyder AG, Fitzgerald P, Wynosky-Dolfi MA, Zwack EE, Hu B, Fitzgerald L, Mauldin EA, Copenhaver AM, Shin S, Wei L, Parker M, Zhang J, Oberst A, Green DR, Brodsky IE. 2014. Caspase-8 mediates caspase-1 processing and innate immune defense in response to bacterial blockade of NF- B and MAPK signaling. Proc Natl Acad Sci 111:7385–7390.
45. Brodsky IE, Palm NW, Sadanand S, Ryndak MB, Sutterwala FS, Flavell RA, Bliska JB, Medzhitov R. 2010. A Yersinia effector protein promotes virulence by preventing inflammasome recognition of the type III secretion system. Cell Host Microbe 7:376–387.
46. Chung LK, Park YH, Zheng Y, Brodsky IE, Hearing P, Kastner DL, Chae JJ, Bliska JB. 2016. The Yersinia Virulence Factor YopM Hijacks Host Kinases to Inhibit Type III Effector-Triggered Activation of the Pyrin Inflammasome. Cell Host Microbe 20:296–306.
47. Lopes Fischer N, Naseer N, Shin S, Brodsky IE. 2020. Effector-triggered immunity and pathogen sensing in metazoans. Nat Microbiol 5:14–26.
48. Knodler LA, Crowley SM, Sham HP, Yang H, Wrande M, Ma C, Ernst RK, Steele-Mortimer O, Celli J, Vallance BA. 2014. Noncanonical inflammasome activation of caspase-4/caspase-11 mediates epithelial defenses against enteric bacterial pathogens. Cell Host Microbe 16:249–256.
49. Naseer N, Zhang J, Bauer R, Constant DA, Nice TJ, Brodsky IE, Rauch I, Shin S. 2022. Salmonella enterica Serovar Typhimurium Induces NAIP/NLRC4- And NLRP3/ASC-Independent, Caspase-4-Dependent Inflammasome Activation in Human Intestinal Epithelial Cells. Infect Immun 90.
50. Matsuura M, Takahashi H, Watanabe H, Saito S, Kawahara K. 2010. Immunomodulatory effects of Yersinia pestis lipopolysaccharides on human macrophages. Clin Vaccine Immunol 17:49–55.
51. Montminy SW, Khan N, McGrath S, Walkowicz MJ, Sharp F, Conlon JE, Fukase K, Kusumoto S, Sweet C, Miyake K, Akira S, Cotter RJ, Goguen JD, Lien E. 2006. Virulence factors of Yersinia pestis are overcome by a strong lipopolysaccharide response. Nat Immunol 7:1066–1073.
52. Hajjar AM, Tsai JH, Wilson CB, Miller SI. 2002. Human Toll-like receptor 4 recognizes host-specific LPS modifications. Nat Immunol 3:354–359.
53. Luchetti G, Roncaioli JL, Chavez RA, Kayagaki N, Vance RE, Dixit Correspondence VM,

850 Schubert AF, Kofoed EM, Reja R, Cheung TK, Liang Y, Webster JD, Lehoux I,
851 Skippington E, Reeder J, Haley B, Tan MW, Rose CM, Newton K, Dixit VM. 2021. In brief
852 Shigella ubiquitin ligase IpaH7.8 targets gasdermin D for degradation to prevent
853 pyroptosis and enable infection The pore-forming protein gasdermin. Cell Host Microbe
854 29.
855 54. Alexander-Floyd J, Bass AR, Harberts EM, Grubaugh D, Buxbaum JD, Brodsky IE, Ernst
856 RK, Shin S. 2022. Lipid A Variants Activate Human TLR4 and the Noncanonical
857 Inflammasome Differently and Require the Core Oligosaccharide for Inflammasome
858 Activation. Infect Immun 90.
859 55. Harberts EM, Grubaugh D, Akuma DC, Shin S, Ernst RK, Brodsky IE. 2022. Position-
860 Specific Secondary Acylation Determines Detection of Lipid A by Murine TLR4 and
861 Caspase-11. Infect Immun 90.
862 56. Sarhan J, Liu BC, Muendlein HI, Li P, Nilson R, Tang AY, Rongvaux A, Bunnell SC, Shao
863 F, Green DR, Poltorak A. 2018. Caspase-8 induces cleavage of gasdermin D to elicit
864 pyroptosis during Yersinia infection. Proc Natl Acad Sci U S A 115:E10888–E10897.
865 57. Valeria MRR, Ramirez J, Naseer N, Palacio NM, Siddarthan IJ, Yan BM, Boyer MA,
866 Pensinger DA, Sauer JD, Shin S. 2017. Broad detection of bacterial type III secretion
867 system and flagellin proteins by the human NAIP/NLRC4 inflammasome. Proc Natl Acad
868 Sci U S A 114:13242–13247.
869 58. Naseer N, Egan MS, Reyes Ruiz VM, Scott WP, Hunter EN, Demissie T, Rauch I,
870 Brodsky IE, Shin S. 2022. Human NAIP/NLRC4 and NLRP3 inflammasomes detect
871 Salmonella type III secretion system activities to restrict intracellular bacterial replication.
872 PLoS Pathog 18.
873 59. Gram AM, Wright JA, Pickering RJ, Lam NL, Booty LM, Webster SJ, Bryant CE. 2021.
874 Salmonella Flagellin Activates NAIP/NLRC4 and Canonical NLRP3 Inflammasomes in
875 Human Macrophages. J Immunol 206:631–640.
876 60. Kobayashi T, Ogawa M, Sanada T, Mimuro H, Kim M, Ashida H, Akakura R, Yoshida M,
877 Kawalec M, Reichhart JM, Mizushima T, Sasakawa C. 2013. The Shigella OspC3 effector
878 inhibits caspase-4, antagonizes inflammatory cell death, and promotes epithelial
879 infection. Cell Host Microbe 13:570–583.
880 61. Egan MS, Zhang J, Shin S. 2023. Human and mouse NAIP/NLRC4 inflammasome
881 responses to bacterial infection. Curr Opin Microbiol 73:102298.
882 62. Sellin ME, Müller AA, Felmy B, Dolowschiak T, Diard M, Tardivel A, Maslowski KM, Hardt
883 WD. 2014. Epithelium-intrinsic NAIP/NLRC4 inflammasome drives infected enterocyte
884 expulsion to restrict salmonella replication in the intestinal mucosa. Cell Host Microbe
885 16:237–248.
886 63. Hausmann A, Böck D, Geiser P, Berthold DL, Fattinger SA, Furter M, Bouman JA,
887 Barthel-Scherrer M, Lang CM, Bakkeren E, Kolinko I, Diard M, Bumann D, Slack E,
888 Regoes RR, Pilhofer M, Sellin ME, Hardt W-D. 2020. Intestinal epithelial NAIP/NLRC4
889 restricts systemic dissemination of the adapted pathogen Salmonella Typhimurium due to
890 site-specific bacterial PAMP expression. Mucosal Immunol
891 https://doi.org/10.1038/s41385-019-0247-0.
892 64. Rauch I, Deets KA, Ji DX, von Moltke J, Tenthorey JL, Lee AY, Philip NH, Ayres JS,
893 Brodsky IE, Gronert K, Vance RE. 2017. NAIP-NLRC4 Inflammasomes Coordinate
894 Intestinal Epithelial Cell Expulsion with Eicosanoid and IL-18 Release via Activation of
895 Caspase-1 and -8. Immunity 46:649–659.
896 65. Mitchell PS, Roncaioli JL, Turcotte EA, Goers L, Chavez RA, Lee AY, Lesser CF, Rauch
897 I, Vance RE. 2020. Naip–nlrc4-deficient mice are susceptible to shigellosis. Elife 9:1–25.
898 66. Roncaioli JL, Babirye JP, Chavez RA, Liu FL, Turcotte EA, Lee AY, Lesser CF, Vance
899 RE. 2022. A hierarchy of cell death pathways confers layered resistance to shigellosis in
900 mice. bioRxiv 2022.09.21.508939.

901 67. Pallett MA, Crepin VF, Serafini N, Habibzay M, Kotik O, Sanchez-Garrido J, Di Santo JP,
902 Shenoy AR, Berger CN, Frankel G. 2016. Bacterial virulence factor inhibits caspase-4/11
903 activation in intestinal epithelial cells. Mucosal Immunol 2017 103 10:602–612.
904 68. Steeghs L, Keestra AM, Van Mourik A, Uronen-Hansson H, Van Der Ley P, Callard R,
905 Klein N, Van Putten JPM. 2008. Differential activation of human and mouse Toll-like
906 receptor 4 by the adjuvant candidate LpxL1 of Neisseria meningitidis. Infect Immun
907 76:3801–3807.
908 69. Lei-Leston AC, Murphy AG, Maloy KJ. 2017. Epithelial Cell Inflammasomes in Intestinal
909 Immunity and Inflammation. Front Immunol 8:1168.
910 70. Marra A, Isberg RR. 1997. Invasin-dependent and invasin-independent pathways for
911 translocation of Yersinia pseudotuberculosis across the Peyer's patch intestinal
912 epithelium. Infect Immun 65:3412–3421.
913 71. Clark MA, Hirst BH, Jepson MA. 1998. M-cell surface β1 integrin expression and invasin-
914 mediated targeting of Yersinia pseudotuberculosis to mouse Peyer's patch M cells. Infect
915 Immun 66:1237–1243.
916 72. Isberg RR, Leong JM. 1990. Multiple beta 1 chain integrins are receptors for invasin, a
917 protein that promotes bacterial penetration into mammalian cells. Cell 60:861–871.
918 73. Autenrieth IB, Firsching R. 1996. Penetration of M cells and destruction of Peyer's
919 patches by Yersinia enterocolitica: an ultrastructural and histological study. J Med
920 Microbiol 44:285–294.
921 74. Sorobetea D, Matsuda R, Peterson ST, Grayczyk JP, Rao I, Krespan E, Lanza M,
922 Assenmacher C-A, Mack M, Beiting DP, Radaelli E, Brodsky IE. 2023. Inflammatory
923 monocytes promote granuloma control of Yersinia infection. Nat Microbiol 1–13.
924 75. Ashida H, Mimuro H, Ogawa M, Kobayashi T, Sanada T, Kim M, Sasakawa C. 2011. Cell
925 death and infection: A double-edged sword for host and pathogen survival. J Cell Biol
926 195:931–942.
927 76. Fink SL, Cookson BT. 2007. Pyroptosis and host cell death responses during Salmonella
928 infection. Cell Microbiol 9:2562–2570.
929 77. Thinwa J, Segovia JA, Bose S, Dube PH. 2014. Integrin-Mediated First Signal for
930 Inflammasome Activation in Intestinal Epithelial Cells. J Immunol 193:1373–1382.
931 78. Denecker G, Declercq W, Geuijen CAW, Boland A, Benabdillah R, Van Gurp M, Sory
932 MP, Vandenabeele P, Cornelis GR. 2001. Yersinia enterocolitica YopP-induced
933 apoptosis of macrophages involves the apoptotic signaling cascade upstream of bid. J
934 Biol Chem 276:19706–19714.
935 79. Lilo S, Zheng Y, Bliska JB. 2008. Caspase-1 activation in macrophages infected with
936 Yersinia pestis KIM requires the type III secretion system effector YopJ. Infect Immun
937 76:3911–3923.
938 80. Spinner JL, Seo KS, O'Loughlin JL, Cundiff JA, Minnich SA, Bohach GA, Kobayashi SD.
939 2010. Neutrophils Are Resistant to Yersinia YopJ/P-Induced Apoptosis and Are Protected
940 from ROS-Mediated Cell Death by the Type III Secretion System. PLoS One 5:e9279.
941 81. Man SM, Hopkins LJ, Nugent E, Cox S, Glück IM, Tourlomousis P, Wright JA, Cicuta P,
942 Monie TP, Bryant CE. 2014. Inflammasome activation causes dual recruitment of NLRC4
943 and NLRP3 to the same macromolecular complex. Proc Natl Acad Sci U S A 111:7403–
944 7408.
945 82. Sarhan J, Liu BC, Muendlein HI, Li P, Nilson R, Tang AY, Rongvaux A, Bunnell SC, Shao
946 F, Green DR, Poltorak A. 2018. Caspase-8 induces cleavage of gasdermin D to elicit
947 pyroptosis during Yersinia infection. Proc Natl Acad Sci U S A 115:E10888–E10897.
948 83. Weng D, Marty-Roix R, Ganesan S, Proulx MK, Vladimer GI, Kaiser WJ, Mocarski ES,
949 Pouliot K, Chan FKM, Kelliher MA, Harris PA, Bertin J, Gough PJ, Shayakhmetov DM,
950 Goguen JD, Fitzgerald KA, Silverman N, Lien E. 2014. Caspase-8 and RIP kinases
951 regulate bacteria-induced innate immune responses and cell death. Proc Natl Acad Sci U

952 S A 111:7391–7396.
953 84. Antonopoulos C, Russo HM, El Sanadi C, Martin BN, Li X, Kaiser WJ, Mocarski ES,
954 Dubyak GR. 2015. Caspase-8 as an Effector and Regulator of NLRP3 Inflammasome
955 Signaling. J Biol Chem 290:20167–20184.
956 85. Bass A. 2020. Elucidating Human Inflammasome Responses To Legionella Pneumophila
957 And Lipopolysaccharide Variants. Publicly Access Penn Diss.
958 86. Agard NJ, Maltby D, Wells JA. 2010. Inflammatory stimuli regulate caspase substrate
959 profiles. Mol Cell Proteomics 9:880–893.
960 87. He WT, Wan H, Hu L, Chen P, Wang X, Huang Z, Yang ZH, Zhong CQ, Han J. 2015.
961 Gasdermin D is an executor of pyroptosis and required for interleukin-1β secretion. Cell
962 Res 2015 2512 25:1285–1298.
963 88. Liu X, Zhang Z, Ruan J, Pan Y, Magupalli VG, Wu H, Lieberman J. 2016. Inflammasome-
964 activated gasdermin D causes pyroptosis by forming membrane pores. Nat 2016
965 5357610 535:153–158.
966 89. Sborgi L, Rühl S, Mulvihill E, Pipercevic J, Heilig R, Stahlberg H, Farady CJ, Müller DJ,
967 Broz P, Hiller S. 2016. GSDMD membrane pore formation constitutes the mechanism of
968 pyroptotic cell death. EMBO J 35:1766–1778.
969 90. Ding J, Wang K, Liu W, She Y, Sun Q, Shi J, Sun H, Wang DC, Shao F. 2016. Pore-
970 forming activity and structural autoinhibition of the gasdermin family. Nat 2016 5357610
971 535:111–116.
972 91. Aglietti RA, Estevez A, Gupta A, Ramirez MG, Liu PS, Kayagaki N, Ciferri C, Dixit VM,
973 Dueber EC. 2016. GsdmD p30 elicited by caspase-11 during pyroptosis forms pores in
974 membranes. Proc Natl Acad Sci U S A 113:7858–7863.
975 92. Hu JJ, Liu X, Xia S, Zhang Z, Zhang Y, Zhao J, Ruan J, Luo X, Lou X, Bai Y, Wang J,
976 Hollingsworth LR, Magupalli VG, Zhao L, Luo HR, Kim J, Lieberman J, Wu H. 2020. FDA-
977 approved disulfiram inhibits pyroptosis by blocking gasdermin D pore formation. Nat
978 Immunol 2020 217 21:736–745.
979 93. Kummer JA, Broekhuizen R, Everett H, Agostini L, Kuijk L, Martinon F, Van Bruggen R,
980 Rg Tschopp J. Inflammasome Components NALP 1 and 3 Show Distinct but Separate
981 Expression Profiles in Human Tissues Suggesting a Site-specific Role in the
982 Inflammatory Response https://doi.org/10.1369/jhc.6A7101.2006.
983 94. Sellin ME, Maslowski KM, Maloy KJ, Hardt WD. 2015. Inflammasomes of the intestinal
984 epithelium. Trends Immunol 36:442–450.
985 95. Dersch P, Isberg RR. 2000. An Immunoglobulin Superfamily-Like Domain Unique to the
986 Yersinia pseudotuberculosis Invasin Protein Is Required for Stimulation of Bacterial
987 Uptake via Integrin Receptors. Infect Immun 68:2930.
988 96. Isberg RR. 1989. Determinants for thermoinducible cell binding and plasmid-encoded
989 cellular penetration detected in the absence of the Yersinia pseudotuberculosis invasin
990 protein. Infect Immun 57:1998–2005.
991 97. Isberg RR, Tran Van Nhieu G. 1994. Binding and internalization of microorganisms by
992 integrin receptors. Trends Microbiol 2:10–14.
993 98. Fallman M, Andersson K, Hakansson S, Magnusson KE, Stendahl O, Wolf- Watz H.
994 1995. Yersinia pseudotuberculosis inhibits Fc receptor-mediated phagocytosis in J774
995 cells. Infect Immun 63:3117–3124.
996 99. Bliska JB, Copass MC, Falkow S. 1993. The Yersinia pseudotuberculosis adhesin YadA
997 mediates intimate bacterial attachment to and entry into HEp-2 cells. Infect Immun
998 61:3914–3921.
999 100. Rosqvist R, Forsberg, Rimpiläinen M, Bergman T, Wolf-Watz H. 1990. The cytotoxic
1000 protein YopE of Yersinia obstructs the primary host defence. Mol Microbiol 4:657–667.
1001 101. Andersson K, Carballeira N, Magnusson KE, Persson C, Stendahl O, Wolf-Watz H,
1002 Fällman M. 1996. YopH of Yersinia pseudotuberculosis interrupts early phosphotyrosine

1003 signalling associated with phagocytosis. Mol Microbiol 20:1057–1069.
1004 102. Black DS, Bliska JB. 2000. The RhoGAP activity of the Yersinia pseudotuberculosis
1005 cytotoxin YopE is required for antiphagocytic function and virulence. Mol Microbiol
1006 37:515–527.
1007 103. Cornelis GR. 2002. The Yersinia Ysc–Yop "Type III" weaponry. Nat Rev Mol Cell Biol
1008 2002 310 3:742–753.
1009 104. Fasciano AC, Dasanayake GS, Estes MK, Zachos NC, Breault DT, Isberg RR, Tan S,
1010 Mecsas J. 2021. Yersinia pseudotuberculosis YopE prevents uptake by M cells and
1011 instigates M cell extrusion in human ileal enteroid-derived monolayers. Gut Microbes 13.
1012 105. Black DS, Bliska JB. 1997. Identification of p130Cas as a substrate of Yersinia YopH
1013 (Yop51), a bacterial protein tyrosine phosphatase that translocates into mammalian cells
1014 and targets focal adhesions. EMBO J 16:2730–2744.
1015 106. Persson C, Carballeira N, Wolf-Watz H, Fällman M. 1997. The PTPase YopH inhibits
1016 uptake of Yersinia, tyrosine phosphorylation of p130Cas and FAK, and the associated
1017 accumulation of these proteins in peripheral focal adhesions. EMBO J 16:2307–2318.
1018 107. Hamid N, Gustavsson A, Andersson K, McGee K, Persson C, Rudd CE, Fällman M.
1019 1999. YopH dephosphorylates Cas and Fyn-binding protein in macrophages. Microb
1020 Pathog 27:231–242.
1021 108. Rosqvist R, Forsberg A, Wolf-Watz H. 1991. Intracellular targeting of the Yersinia YopE
1022 cytotoxin in mammalian cells induces actin microfilament disruption. Infect Immun
1023 59:4562.
1024 109. Viboud GI, Bliska JB. 2001. A bacterial type III secretion system inhibits actin
1025 polymerization to prevent pore formation in host cell membranes. EMBO J 20:5373–
1026 5382.
1027 110. Wong KW, Mohammadi S, Isberg RR. 2008. The Polybasic Region of Rac1 Modulates
1028 Bacterial Uptake Independently of Self-association and Membrane Targeting. J Biol
1029 Chem 283:35954.
1030 111. Wong KW, Isberg RR. 2005. Yersinia pseudotuberculosis Spatially Controls Activation
1031 and Misregulation of Host Cell Rac1. PLOS Pathog 1:e16.
1032 112. Alrutz MA, Srivastava A, Wong KW, D'Souza-Schorey C, Tang M, Ch'ng LE, Snapper
1033 SB, Isberg RR. 2001. Efficient uptake of Yersinia pseudotuberculosis via integrin
1034 receptors involves a Rac1-Arp 2/3 pathway that bypasses N-WASP function. Mol
1035 Microbiol 42:689–703.
1036 113. Rottner K, Stradal TEB, Wehland J. 2005. Bacteria-host-cell interactions at the plasma
1037 membrane: stories on actin cytoskeleton subversion. Dev Cell 9:3–17.
1038 114. Ridley AJ. 2006. Rho GTPases and actin dynamics in membrane protrusions and vesicle
1039 trafficking. Trends Cell Biol 16:522–529.
1040 115. Parsons JT. 2003. Focal adhesion kinase: the first ten years. J Cell Sci 116:1409–1416.
1041 116. Uliczka F, Kornprobst T, Eitel J, Schneider D, Dersch P. 2009. Cell invasion of Yersinia
1042 pseudotuberculosis by invasin and YadA requires protein kinase C, phospholipase C-γ1
1043 and Akt kinase. Cell Microbiol 11:1782–1801.
1044 117. Eitel J, Dersch P. 2002. The YadA Protein of Yersinia pseudotuberculosis Mediates High-
1045 Efficiency Uptake into Human Cells under Environmental Conditions in Which Invasin Is
1046 Repressed. Infect Immun 70:4880.
1047 118. Isberg RR, Voorhis DL, Falkow S. 1987. Identification of invasin: a protein that allows
1048 enteric bacteria to penetrate cultured mammalian cells. Cell 50:769–778.
1049 119. Maldonado-Arocho FJ, Green C, Fisher ML, Paczosa MK, Mecsas J. 2013. Adhesins and
1050 Host Serum Factors Drive Yop Translocation by Yersinia into Professional Phagocytes
1051 during Animal Infection. PLoS Pathog 9.
1052 120. Simonet M, Falkow S. 1992. Invasin expression in Yersinia pseudotuberculosis. Infect
1053 Immun 60:4414–4417.

1054 121. de Rouvroit CL, Sluiters C, Cornelis GR. 1992. Role of the transcriptional activator, VirF,
1055 and temperature in the expression of the pYV plasmid genes of Yersinia enterocolitica.
1056 Mol Microbiol 6:395–409.
1057 122. Sharma D, Malik A, Guy CS, Karki R, Vogel P, Kanneganti TD. 2018. Pyrin
1058 Inflammasome Regulates Tight Junction Integrity to Restrict Colitis and Tumorigenesis.
1059 Gastroenterology 154:948.
1060 123. Saavedra PHV, Huang L, Ghazavi F, Kourula S, Vanden Berghe T, Takahashi N,
1061 Vandenabeele P, Lamkanfi M. 2018. Apoptosis of intestinal epithelial cells restricts
1062 Clostridium difficile infection in a model of pseudomembranous colitis. Nat Commun 9.
1063 124. Pentecost M, Kumaran J, Ghosh P, Amieva MR. 2010. Listeria monocytogenes Internalin
1064 B Activates Junctional Endocytosis to Accelerate Intestinal Invasion. PLoS Pathog
1065 6:1000900.
1066 125. McCormick BA, Nusrat A, Parkos CA, D'Andrea L, Hofman PM, Carnes D, Liang TW,
1067 Madara JL. 1997. Unmasking of intestinal epithelial lateral membrane β1 integrin
1068 consequent to transepithelial neutrophil migration in vitro facilitates inv- mediated
1069 invasion by Yersinia pseudotuberculosis. Infect Immun 65:1414–1421.
1070 126. Tafazoli F, Holmstrom A, Forsberg A, Magnusson KE. 2000. Apically exposed, tight
1071 junction-associated beta1-integrins allow binding and YopE-mediated perturbation of
1072 epithelial barriers by wild-type Yersinia bacteria. Infect Immun 68:5335–5343.
1073 127. Feeley EM, Pilla-Moffett DM, Zwack EE, Piro AS, Finethy R, Kolb JP, Martinez J, Brodsky
1074 IE, Coers J. 2017. Galectin-3 directs antimicrobial guanylate binding proteins to vacuoles
1075 furnished with bacterial secretion systems. Proc Natl Acad Sci U S A 114:E1698–E1706.
1076 128. Zhang Y, Murtha J, Roberts MA, Siegel RM, Bliska JB. 2008. Type III secretion
1077 decreases bacterial and host survival following phagocytosis of Yersinia
1078 pseudotuberculosis by macrophages. Infect Immun 76:4299–4310.
1079 129. Livak KJ, Schmittgen TD. 2001. Analysis of Relative Gene Expression Data Using Real-
1080 Time Quantitative PCR and the 2−ΔΔCT Method. Methods 25:402–408.
1081 130. Viboud GI, So SSK, Ryndak MB, Bliska JB. 2003. Proinflammatory signalling stimulated
1082 by the type III translocation factor YopB is counteracted by multiple effectors in epithelial
1083 cells infected with Yersinia pseudotuberculosis. Mol Microbiol 47:1305–1315.
1084 131. Ryndak MB, Chung H, London E, Bliska JB. 2005. Role of predicted transmembrane
1085 domains for Type III translocation, pore formation, and signaling by the Yersinia
1086 pseudotuberculosis YopB protein. Infect Immun 73:2433–2443.
1087

Figure 1

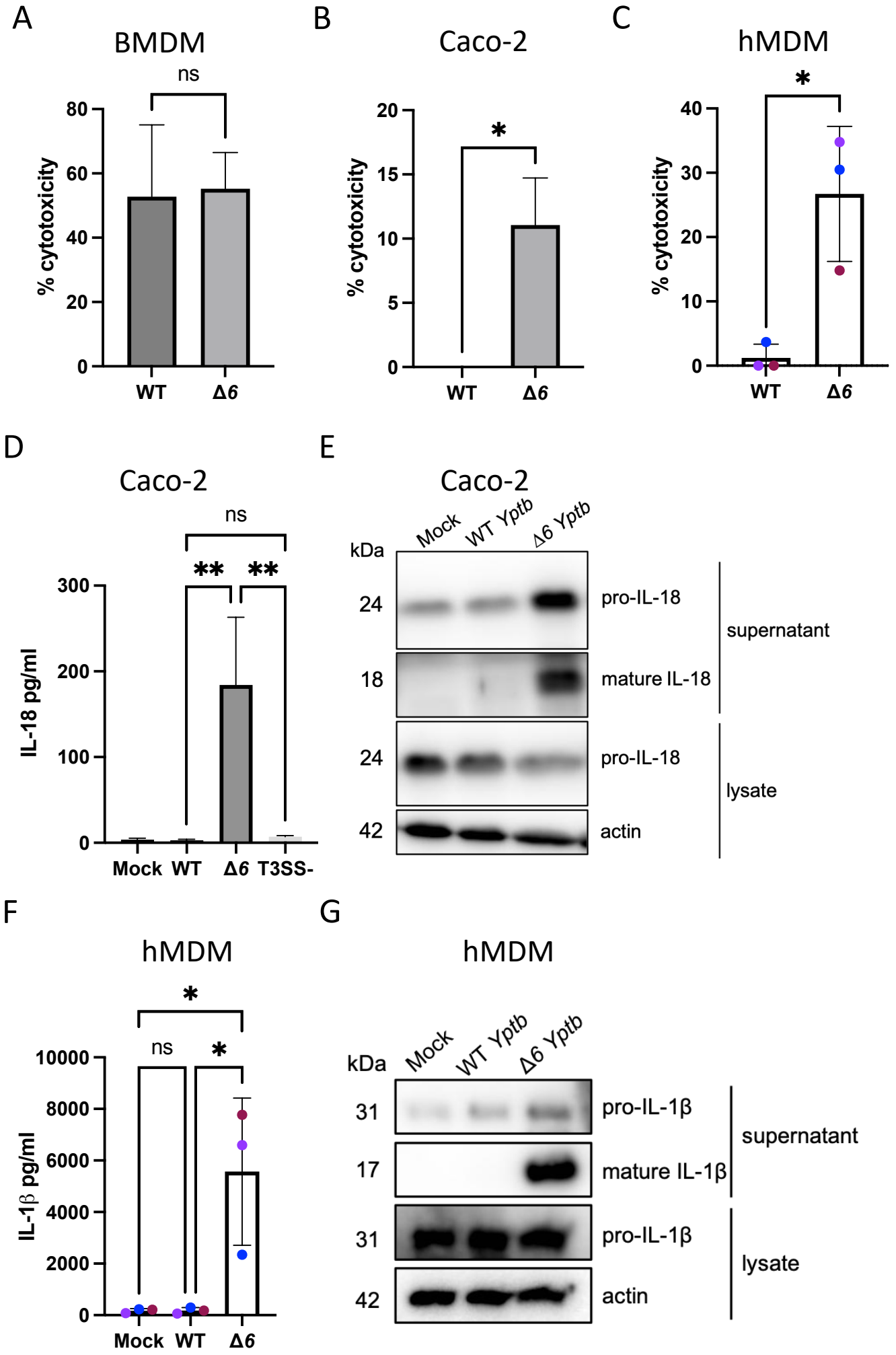
A
BMDM
ns
% cytotoxicity
80
60
40
20
0
WT
Δ6
B
Caco-2
*
% cytotoxicity
20
15
10
5
0
WT
Δ6
C
hMDM
*
% cytotoxicity
40
30
20
10
0
WT
Δ6
D
Caco-2
ns
**
**
IL-18 pg/ml
300
200
100
0
Mock
WT
Δ6
T3SS-
E
Caco-2
Mock
WT Yptb
Δ6 Yptb
kDa
24
pro-IL-18
supernatant
18
mature IL-18
24
pro-IL-18
lysate
42
actin
F
hMDM
*
ns
*
IL-1β pg/ml
10000
8000
6000
4000
2000
0
Mock
WT
Δ6
G
hMDM
Mock
WT Yptb
Δ6 Yptb
kDa
31
pro-IL-1β
supernatant
17
mature IL-1β
31
pro-IL-1β
lysate
42
actin

Figure 2

A

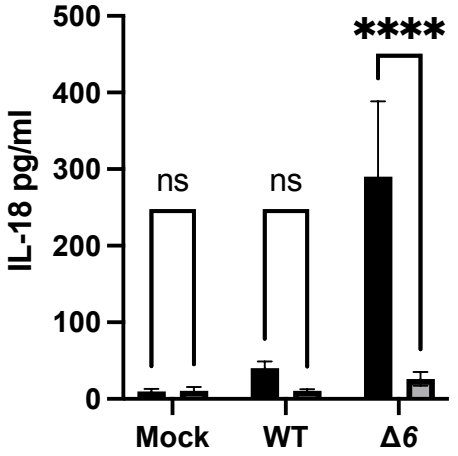

B

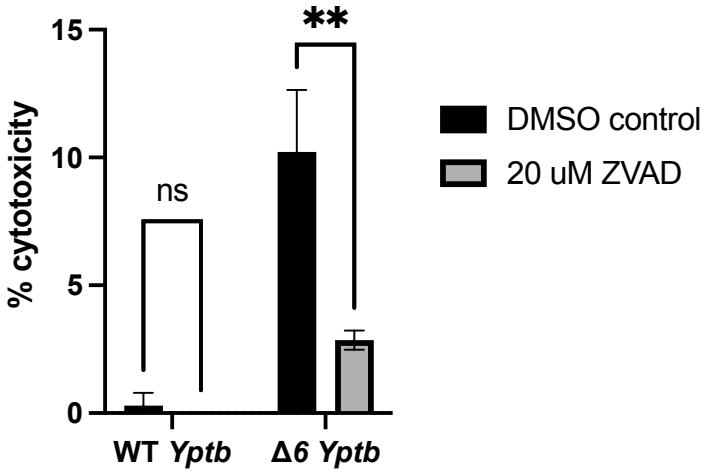

C

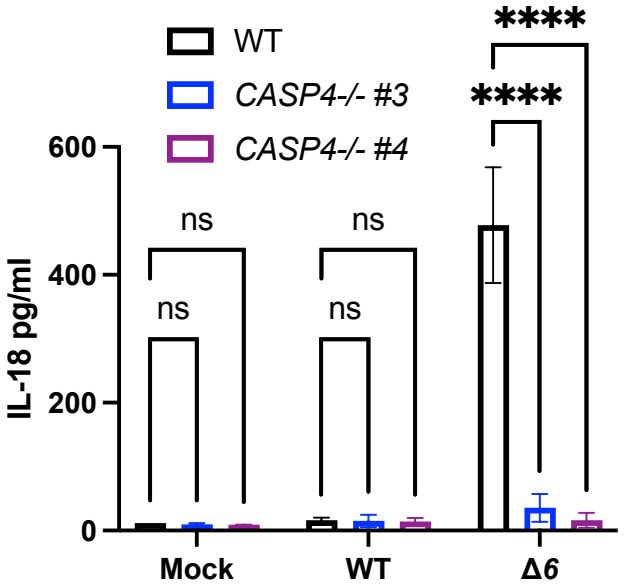

D

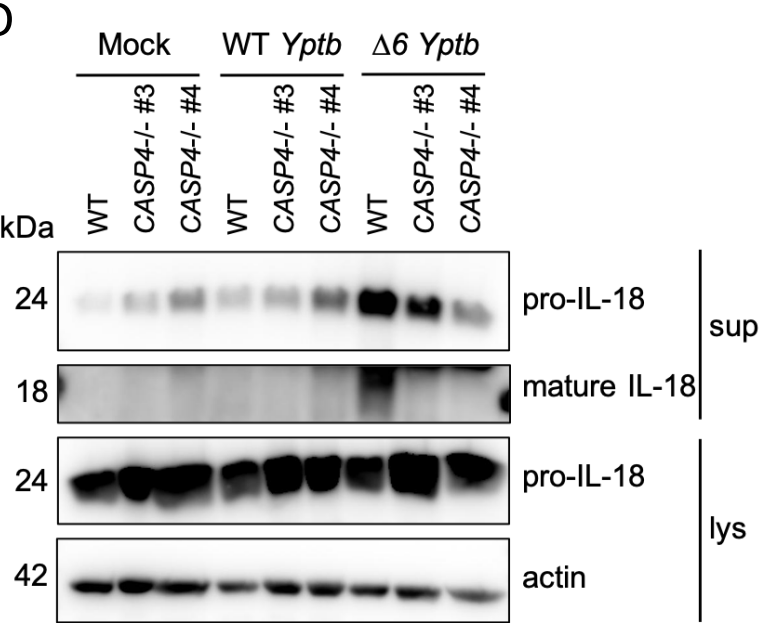

E

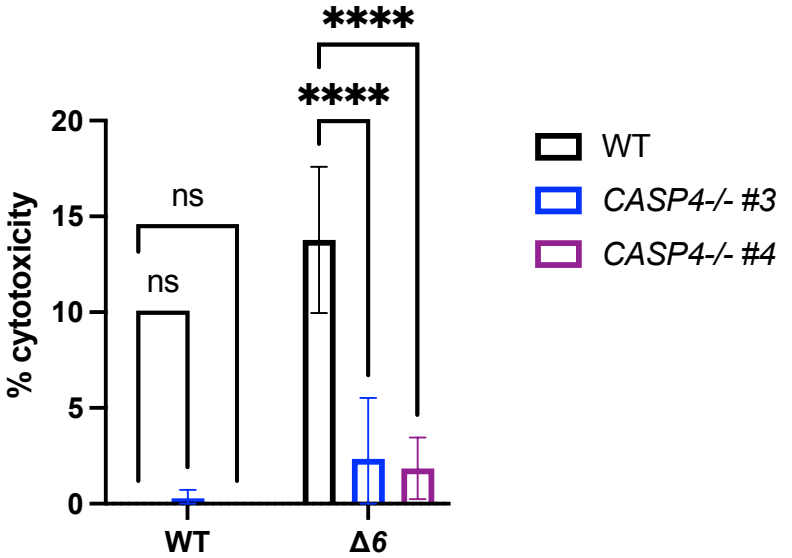

Figure 3

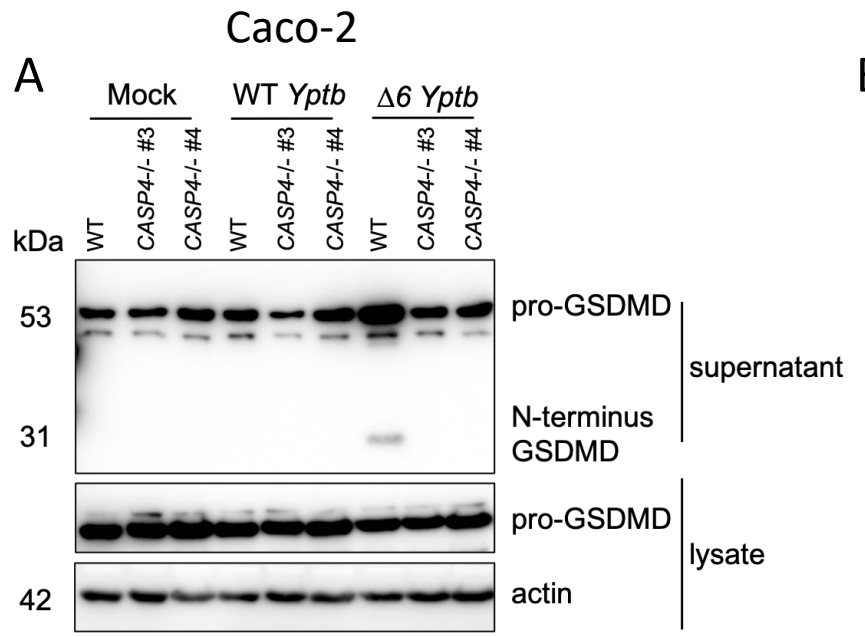
Caco-2
A
Mock
WT Yptb
Δ6 Yptb
WT
CASP4-/- #3
CASP4-/- #4
kDa
53
31
42
pro-GSDMD
N-terminus GSDMD
supernatant
pro-GSDMD
actin
lysate

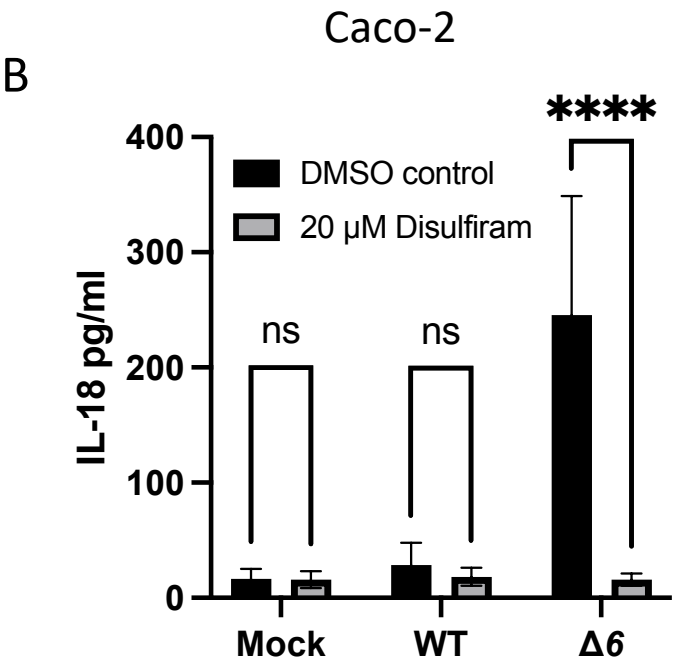
Caco-2
B
IL-18 pg/ml
400
300
200
100
0
DMSO control
20 μM Disulfiram
ns
ns
****
Mock
WT
Δ6

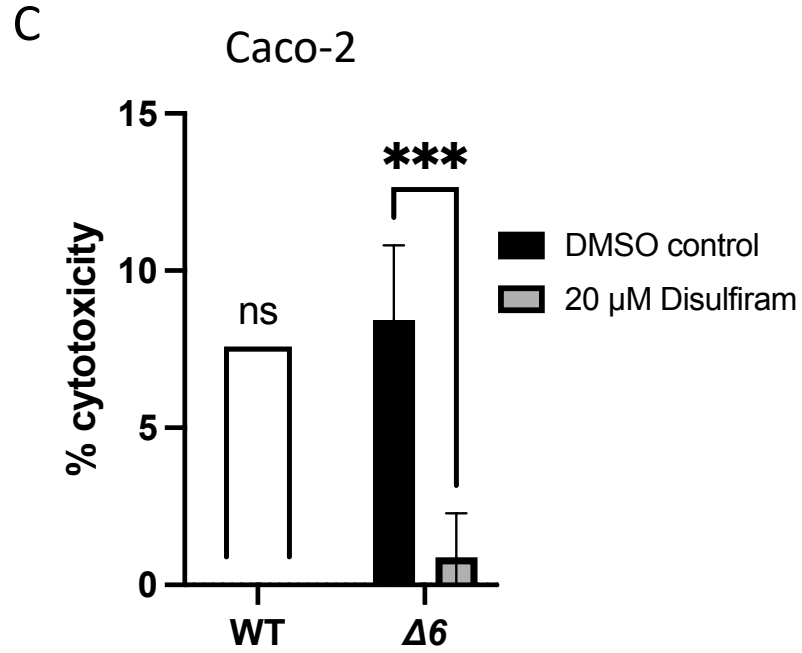
C
Caco-2
% cytotoxicity
15
10
5
0
ns
***
DMSO control
20 μM Disulfiram
WT
Δ6

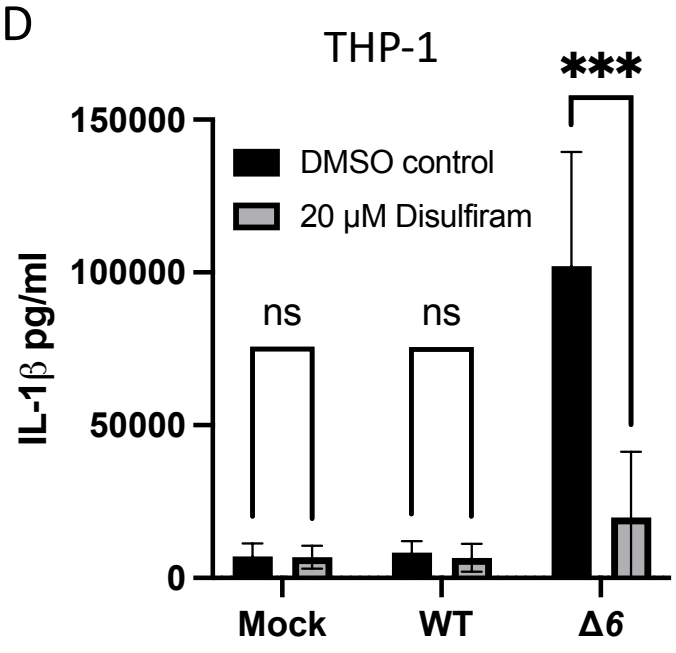
D
THP-1
IL-1β pg/ml
150000
100000
50000
0
DMSO control
20 μM Disulfiram
ns
ns
***
Mock
WT
Δ6

Figure 4

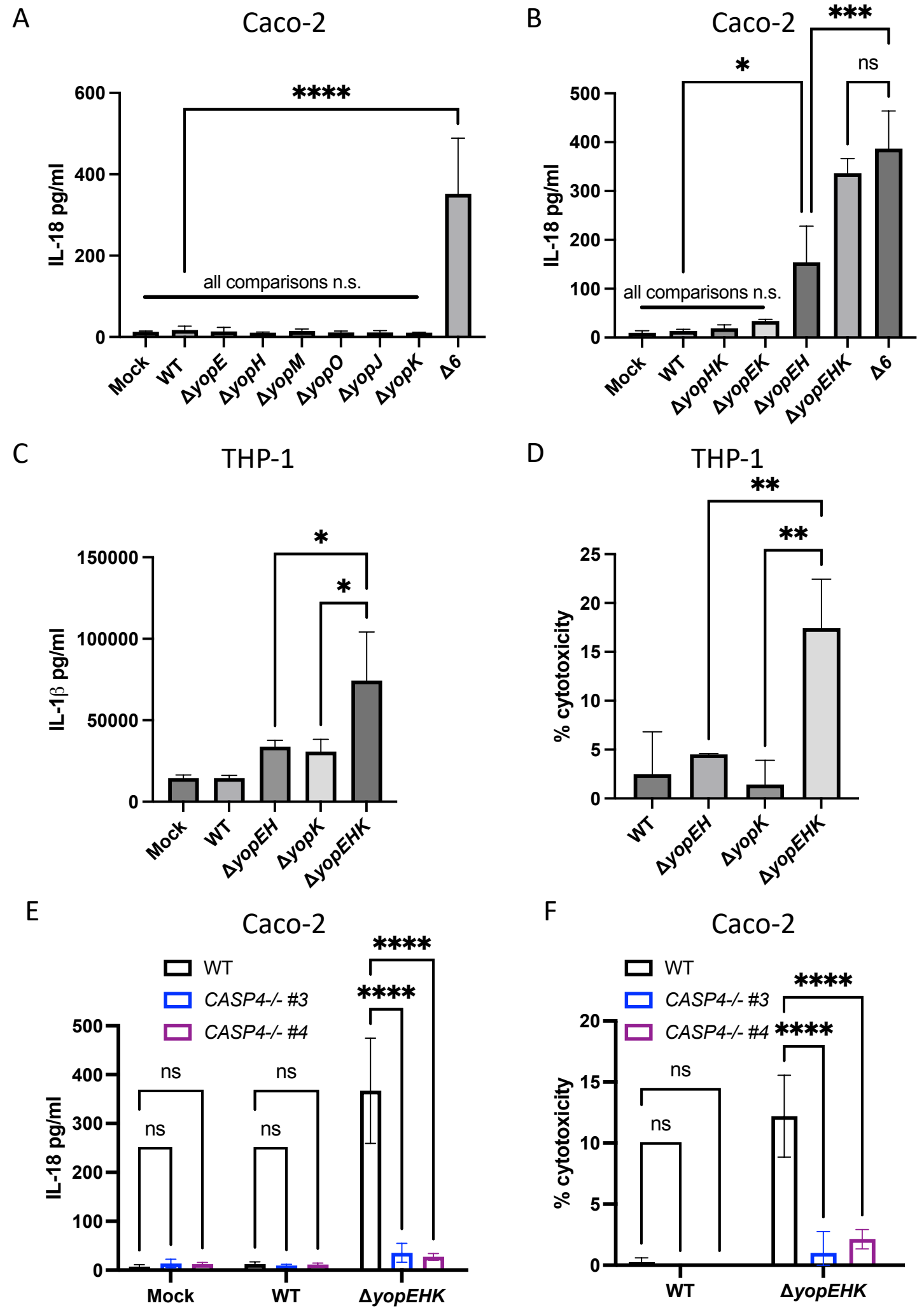
A
Caco-2
IL-18 pg/ml
600
400
200
0
****
all comparisons n.s.
Mock
WT
ΔyopE
ΔyopH
ΔyopM
ΔyopO
ΔyopJ
ΔyopK
Δ6
B
Caco-2
IL-18 pg/ml
500
400
300
200
100
0
*
***
ns
all comparisons n.s.
Mock
WT
ΔyopHK
ΔyopEK
ΔyopEH
ΔyopEHK
Δ6
C
THP-1
IL-1β pg/ml
150000
100000
50000
0
*
*
Mock
WT
ΔyopEH
ΔyopK
ΔyopEHK
D
THP-1
% cytotoxicity
25
20
15
10
5
0
**
**
WT
ΔyopEH
ΔyopK
ΔyopEHK
E
Caco-2
WT
CASP4-/- #3
CASP4-/- #4
IL-18 pg/ml
500
400
300
200
100
0
ns
ns
ns
ns
****
****
Mock
WT
ΔyopEHK
F
Caco-2
WT
CASP4-/- #3
CASP4-/- #4
% cytotoxicity
20
15
10
5
0
ns
ns
****
****
WT
ΔyopEHK

Figure 5

A

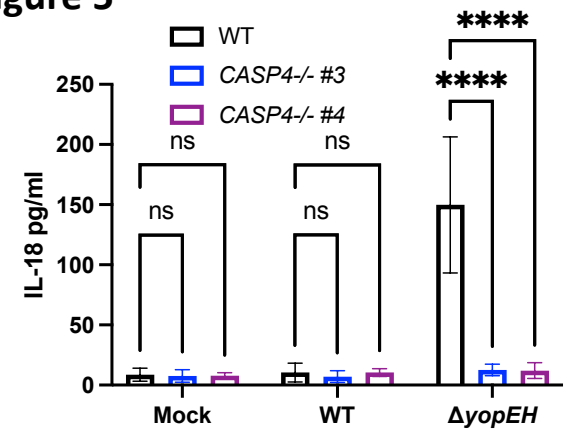

B

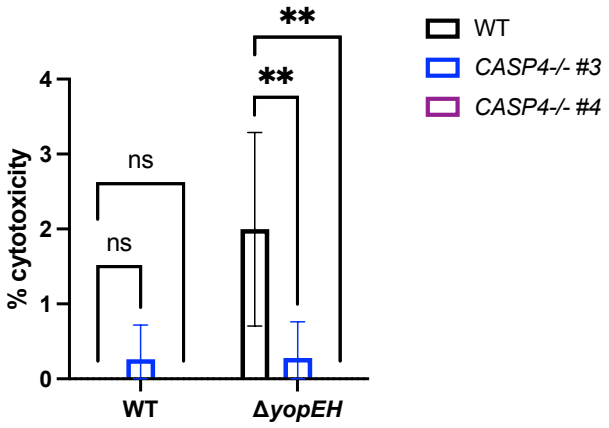

C

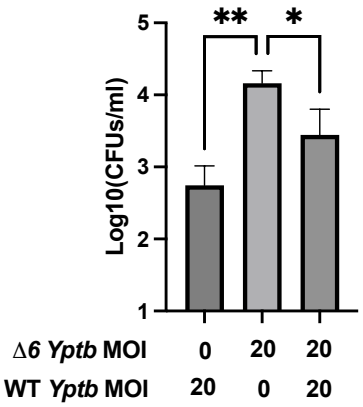

D

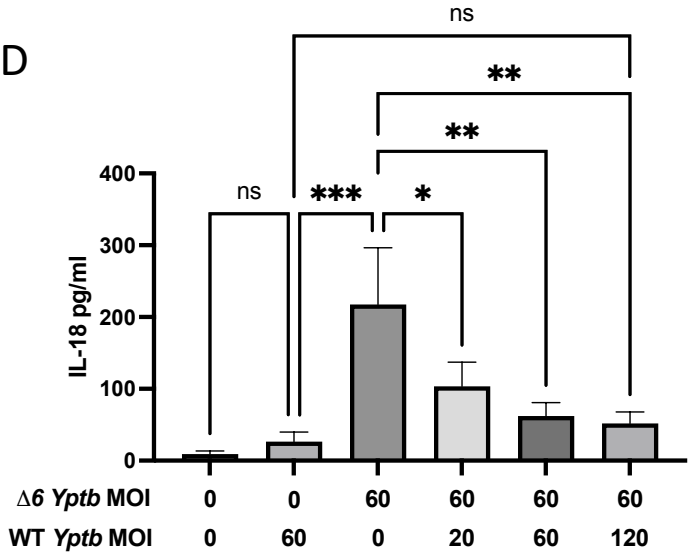

E

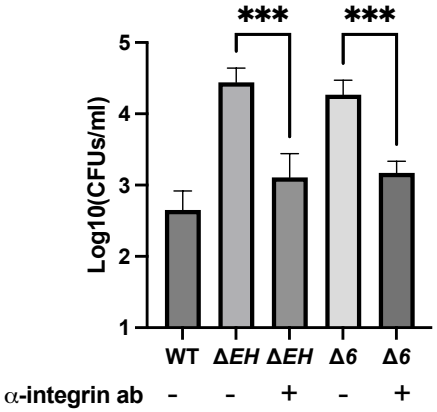

F

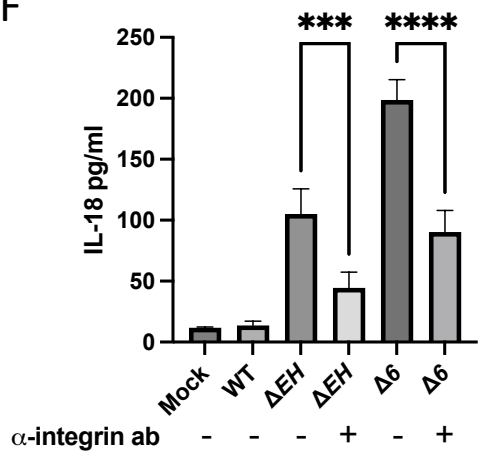

G

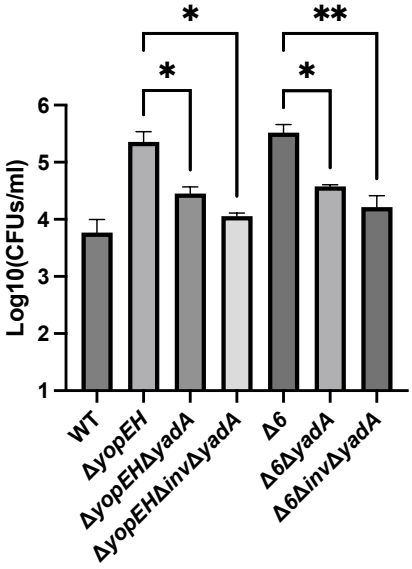
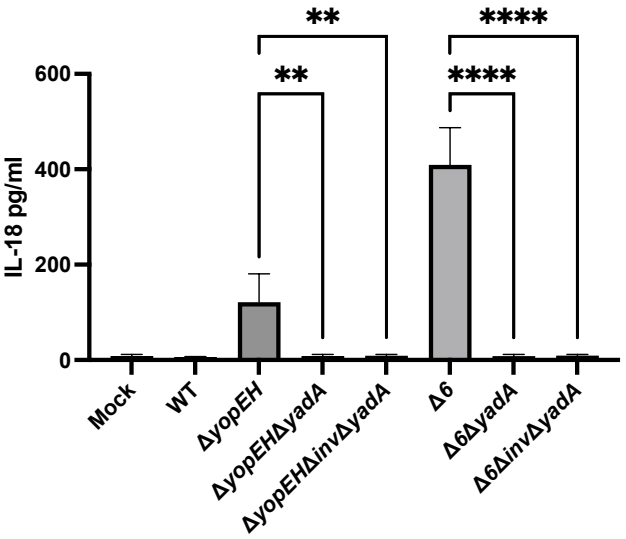
H